Journal of Membrane Science 691 (2024) 122258

Contents lists available at ScienceDirect

Journal of Membrane Science

journal homepage: www.elsevier.com/locate/memsci

Metal- and covalent-organic framework mixed matrix membranes for CO_2 separation: A perspective on stability and scalability

Meixia Shan [a,b,**], Xiumei Geng [a], Inhar Imaz [c], Anna Broto-Ribas [c], Borja Ortín-Rubio [c], Daniel Maspoch [c,d], Luca Ansaloni [e], Thijs A. Peters [e], Alberto Tena [f,g], Marcel E. Boerrigter [h], David A. Vermaas [b,*]

[a] School of Chemical Engineering, Zhengzhou University, Zhengzhou, 450001, PR China
[b] Chemical Engineering Department, Delft University of Technology, van der Maasweg, 9, 2629, HZ Delft, the Netherlands
[c] Catalan Institute of Nanoscience and Nanotechnology (ICN2), CSIC and the Barcelona Institute of Science and Technology, Campus UAB, Bellaterra, 08193, Barcelona, Spain
[d] ICREA, Pg. Lluís Companys 23, 08010, Barcelona, Spain
[e] SINTEF Industry, P.O. Box 124 Blindern, N-0314, Oslo, Norway
[f] Membrane Science and Technology, Faculty of Science and Technology, MESA+ Institute for Nanotechnology, University of Twente, P.O. Box 217, AE Enschede, the Netherlands
[g] Surfaces and Porous Materials (SMAP), Associated Research Unit to CSIC, Institute of Sustainable Processes (ISP), Dr. Mergelina S/n, University of Valladolid, 47071, Valladolid, Spain
[h] LEITAT Technological Center, Carrer de Pallars, 179-185, 08005, Barcelona, Spain

ABSTRACT

Membrane technology has attracted great industrial interest in carbon capture and separation owing to the merits of energy-efficiency, environmental friendliness and low capital investment. Conventional polymeric membranes for CO_2 separation suffer from the trade-off between permeability and selectivity. Introducing porous fillers in polymers is one approach to enhance membrane separation performance. Metal-organic frameworks (MOFs), with ordered porous structure and diverse chemical functionalities, are promising fillers to prepare mixed matrix membranes (MMMs) for CO_2 separation. However, the main issue of MOF based MMMs in industry is their stability and processability. This review analyses recent work on stable and scalable MOF based MMMs for CO_2 separation. The typical stable MOFs, MOF-based MMMs and the scalable MOF synthesis are summarized. A large number of MOF-based MMM suffer from instability upon exposure to contaminants. For that reason, we also discuss the use of covalent organic frameworks (COFs) as an alternative to prepare MMMs for CO_2 separation, considering their excellent stability and good compatibility with polymers. Finally, a brief conclusion and current challenges on obtaining scalable and stable MMMs are outlined. This review may provide some guidance for designing high performance MMMs for industrial CO_2 capture and separation to help achieving carbon neutrality.

1. Introduction

Global warming due to the enhanced and continuing emission of greenhouse gases has caused great public concern. Different approaches are being considered and adopted by various countries to reduce CO_2 emissions, including the potential key carbon capture and storage (CCS) technology [1]. However, the conventional technologies using amine scrubbing or sorbents are facing covdnstraints like scale-up issues, high cost, large footprint, high energy consumption and are potentially environmental unfriendly [2]. Membranes offer a viable energy-saving alternative approach to capture CO_2 due to their versatility, scalability, ease of operation, small footprint and energy efficiency [3]. Nowadays, polymer membranes dominate the membrane market due to the low cost and good processability. For example, the removal of CO_2 from natural gas, the recovery of H_2 (in cracking processes) and oxygen/nitrogen separation using cellulose acetate or polyimide membranes are commercial applications in industry [4,5]. However, the separation performance of polymeric membranes for gas separation obey an intrinsic trade-off relation between permeability and selectivity [6,7]. Furthermore, plasticization and aging issues also restrict their industrial application [8–11]. To overcome the limit of polymer membranes, one pursued method is the preparation of mixed-matrix membranes (MMMs), where inorganic/organic fillers such as carbon molecular sieves (CMSs) [12], carbon nanotubes [13], zeolites [14,15],

---

* Corresponding author. Chemical Engineering Department, Delft University of Technology, van der Maasweg, 9, 2629, HZ Delft, the Netherlands.

** Corresponding author. School of Chemical Engineering, Zhengzhou University, Zhengzhou, 450001, PR China.

E-mail addresses: mxshan@zzu.edu.cn (M. Shan), D.A.Vermaas@tudelft.nl (D.A. Vermaas).

https://doi.org/10.1016/j.memsci.2023.122258
Received 25 September 2023; Received in revised form 5 November 2023; Accepted 7 November 2023

covalent organic frameworks (COFs) [16–18] and metal organic frameworks (MOFs) [19–24] are dispersed in a continuous polymer matrix. MMMs could combine the advantages of both fillers and polymer matrixes, for which selectivity and permeability is observed to surpass the limits of conventional polymer membranes [25–28].

Among the different families of fillers, metal-organic frameworks (MOFs), represent an important class of crystalline molecular sieves that are constructed from linking metal-ions clusters and organic linkers through coordination bonds [29,30]. MOFs are known for their extraordinary structural variability, as both metal ion/clusters and organic linkers can be independently chosen to form MOFs with diverse pore structures and functionalities. MOFs display several advantages over other solid materials, such as permanent porosity with high surface area, flexibility and adjustable pore sizes and tuneable pore surface modifications [31], which enable them as good candidates to be used as fillers in developing novel MMMs [32–36]. Although (idealized) lab-scale experiments have convincingly demonstrated increased selectivity and/or permeability for several MOF-polymer combinations, the large-scale deployment of MOF-based MMM's for CO_2 capture is still awaiting. The development of MOF-based MMMs has been largely restricted by their chemical stability; *e.g.,* ambient moisture or variable pH may result in the degradation of the framework for most of the early MOFs [37–40]. In this context, developing stable-MOF membranes are necessary for real industrial gas separation applications where the feed gas stream may contain trace contaminants such as NO_x, SO_2 or NH_3, specially under humid conditions [41,42].

The diversity and number of MOF structures has grown in recent years, including synthesis of thermally and chemically stable MOFs [43–45], enabling the possibility to be processed into stable MMMs. In addition to stability, process scalability is also a critical factor that needs to be taken into account when choosing MOFs to prepare the MMM: scalability may indeed become the main barrier for membrane commercialization. There have been several previous reviews [46–50], focussing on the performance under idealized lab-conditions. While real conditions require long-term stability and large-scale manufacturing, very few papers [51–55] have assessed upscaled real-life conditions. Instead, a substantial amount of individual works has assessed the stability of MOF-based MMM's in lab-environment.

To assess the practical potential of MOF-based MMMs, this review provides an overview on reported stability of MOF-based MMMs and assess their manufacturability. We aim to provide insight in the stability and manufacturability of MOF-based MMM's in non-idealized conditions and proposed methods for upscaled manufacturability. In this review, we highlight the current progress and identify the future opportunities of stable and scalable MOF based mixed-matrix membranes for CO_2 separation. Due to the challenging stability of MOFs under real-life gas conditions, we also analyse the recent use of covalent-organic frameworks (COFs; analogues of MOFs but made exclusively of organic linkers [56,57]) as a promising type of fillers in MMMs.

2. Framework of industrial conditions for CO_2 capture

Industrial gas streams include contaminants that are typically neglected in lab-scale tests, such as water vapor, hydrocarbons, aromatic compounds and corrosive gases. Table 1 listed the typical contaminate gases in CO_2 capture processes.

In the pre-combustion CO_2 capture process, CO_2 needs to be removed from fossil fuels before combustion is completed. For example, the fossil fuels first undergo partially oxidization in steam and oxygen/air at high pressure and temperature to generate synthesis gas. The syngas obtained after combustion reaction is a mixture of H_2, CO, CO_2 and small amounts of CH_4 [58].

Table 1
The content of typical contaminants in different feed gas.

Feed type	Major gas components	Typical contaminants	Ref.
Pre-combustion CO_2 capture	H_2/CO_2 mixture	H_2O, CO, CH_4, H_2S	[58]
Post-combustion CO_2 capture	CO_2/N_2 mixture	20 wt% moisture, 200–5000 ppmv SOx, 150–300 ppmv NOx, <10 ppmv NO_2, NH_3 (15–50 ppm), HCl (0.5–1 ppm), suspended particulate matter (2–5 mg/Nm^3)	[59]
		30 ppm of SO_2	[60]
		SOx (10–300 mg/Nm^3), NOx (30–280 mg/Nm^3), Dust (<5 mg/Nm^3)	[61]
Upgrading of biogas	CO_2/CH_4 mixture	10–10,000 ppmv (0.0001–1 vol%) H_2S, Traces of H_2S, NH_3, CO, Halogenated carbohydrates	[62]

For post-combustion CO_2 capture applications related to power generation, the gas streams are mainly composed by CO_2 and N_2 with up to 20 wt% moisture, 200–5000 ppmv SOx before desulphurisation (mainly in the form of SO_2 with a small proportion of SO_3) and 150–300 ppmv NOx with NO as main component and <10 ppmv NO_2 [59]. It is important to note that the levels of impurities are dependent on the fuel type used in the combustion. For example, for an advanced supercritical (ASC) pulverized fuel (PF) bituminous power plant, the flue gas after desulphurisation is expected to contain 30 ppm of SO_2 [60]. The content of SO_2 can be further reduced an additional washing step. In the case of post-combustion capture retrofitted to a cement plant, small amount of NH_3 (15–50 ppm), HCl (0.5–1 ppm) and suspended particulate matter (2–5 mg/Nm^3) can also be present in the gaseous stream fed to the separation module [59]. Also with respect to flue gases from the major CO_2 emission sources in an integrated steel mill, SOx (10–300 mg/Nm^3), NOx (30–280 mg/Nm^3) and dust (<5 mg/Nm^3) represent the major contaminants [61]. H_2S is often present in natural gas upgrading (potentially in the %-level, depending on gas field). For upgrading of biogas, traces of H_2S, NH_3, CO and saturated or halogenated carbohydrates can be present. The H_2S content can vary with the organic being composted, but typical values of 10–10,000 ppmv (0.0001–1 vol%) are reported [62].

3. Stability of MOFs to industrial gas stream conditions

3.1. *Stability to humidity*

MOFs could potentially be affected by the presence of water vapor and other gases (NH_3, SO_2 and H_2S) in industrial gas streams. These gaseous contaminants can break the metal-ligand bonds by coordinating to, oxidizing or hydrolyzing the metal centers and/or by protonating the ligands. Thus, MOFs designed for practical CO_2-applications must resist such gases for extended periods of time without suffering any loss in functionality [3]. Unfortunately, there have not yet been any studies evaluating the stability of such MOFs under real conditions of industrial gas streams. The limited number of literature on the stability of MOFs to gases is focused on their hydrolytic stability, although there have been some reports confirming that certain MOFs are stable to pure NH_3, H_2S or SO_2 [63]. These data may help researchers in their design of stable MOFs for industrial-scale CO_2-capture.

Many of the archetypical MOFs used to generate the first MMMs, including HKUST-1, Cr-MIL-101 and MOF-5 (plus some related IRMOFs), are expected not to be stable to water vapor or other industrial gases. For example, these MOFs are not stable to water vapor, which causes their relatively weak metal-oxygen bonds to undergo phase transformation, leading to framework decomposition. This type of decomposition is signalled analytically by degradation or loss of reflection at specific positions in the powder X-ray diffraction (PXRD) pattern; and functionally, by loss in the porosity and gas uptake of the MOF [64–66]. Similarly to water vapor, NH_3 gas reacts with HKUST-1, driving transformations that cause irreversible losses in structure and porosity, as described by Peterson et al. [67] They observed that under dry conditions, this reaction generates a diamine−copper(II) complex, whereas under humid conditions, it generates $Cu(OH)_2$ and $(NH_4)_3BTC$. Such structural damage has obvious functional consequences: for example, Saha and Deng reported that exposure of MOF-5 or *iso*reticular IRMOFs to NH_3 leads to the formation of hydrogen bonds between the Zn_4O centers and NH_3, triggering a massive decrease in the adsorption capacities of each MOF [68]. Furthermore, acidic gases can induce protonation of the metal-bound ligands in MOFs, causing the bonds to break and consequently, to deteriorated MOF performance. This has been reported for reaction of H_2S with ZIF-8 and with HKUST-1; in the latter case, protonation of the trimesic acid ligand leads to framework collapse [69].

The ZIF-type MOFs have been extensively studied. Yaghi et al. [70] reported the highly stable ZIF-8 and -11, demonstrating remarkable chemical resistance towards refluxing organic solvents, water and aqueous alkaline solution. However, Liu et al. [71] observed a different phenomenon that ZIF-8 and other ZIFs (ZIF-7, ZIF-93) underwent hydrolysis under hydrothermal conditions when employing low crystal concentration (0.060 wt%). The authors concluded that ZIF-8 is stable in water at high crystal concentrations due to the protection of its released ligands, which originates from the residuals on the ZIF-8 and (or) few early decomposed ZIF-8. The bare ZIF-8 itself is not stable at 353 K in water and its stability can be highly improved by a shell-ligand –exchange-reaction.

3.2. Stability to other contaminants

The effects of corrosive gas exposure have been studied in other MOFs proposed for CO_2-adsorption applications, including the MOF-74/CPO-27 series, which is built from metal-oxide chains interconnected through 2,5-dioxido-1,4-benzenedicarboxylate linkers. Liu et al. reviewed literature on the effect of water vapor on the CO_2-adsorption capacity of MOF-74 members and concluded that those with less-reductive metal centers are more stable than those possessing more-reductive metal centers: for example, that Ni^{2+}-MOF-74 is more stable to water vapor than is Mg^{2+}-MOF-74 [72]. Similarly, Tan et al. studied the selective co-adsorption capacities of these MOFs towards CO_2 in competition with water vapor, NH_3, SO_2, NO, NO_2, N_2, O_2 and CH_4 [73]. Although they did not observe any framework degradation during the adsorption, they did report that the presence of water vapor was detrimental to the CO_2-uptake capacity of the MOFs, due to the high affinity of their open metal sites for water molecules. For more intuition, we summarize the impact of several contaminants on MOFs in the industrial gas streams in Table 2.

Interestingly, MOFs that contain high-valence metals (*e.g.* Zr^{4+}, $Ti^{4+}$and Al^{3+}, shown in Fig. 1) and broadly-connected nodes bridged by oxo- and hydroxo-groups tend to exhibit relatively high stability to coordinating vapors and gases [74–77]. Among them, there are several MOF families that are known for their hydrolytic stability. These include UiO-type MOFs, which are *iso*reticular MOFs comprising Zr^{4+}-oxide clusters ($Zr_6O_4(OH)_4$) connected through polycarboxylate linkers; several members of MIL MOFs, such as MIL-125(Ti) and MIL-101(Cr); and some Al^{3+}-MOFs built from highly stable, high-nuclearity, oxo-chains, including CAU-10 [78,79]. Remarkably, several studies have shown that some of these MOFs are also stable to H_2S, NH_3 and/or SO_2. For example, Walton et al. demonstrated that UiO-66, MIL-125(Ti) and MIL-101(Cr) are stable to H_2S exposure [78]. They conducted adsorption experiments using multicomponent gas mixtures, including H_2S/CH_4 (1:99 mol/mol) and $H_2S/CO_2/CH_4$ (1:10:89 mol/mol), confirming that the MOFs retained their adsorption capacities. Likewise, Khabzina and co-workers reported that UiO-66_COOH, a UiO-66 analog that contains free carboxylic groups, showed excellent stability to NH_3 [80]. Moreover, Carter et al. found that $[Zr_6(\mu_3\text{-}O)_4(\mu_3\text{-}OH)_4(OH)_4(H_2O)_4(L)_2]$ (also known as *MFM-601*; where L = 4,4′,4″,4‴-(1,4-phenylenebis(pyridine-4,2,6-triyl))tetrabenzoate), could adsorb 12.3 mmol SO_2/g MOF without any signs of degradation [81]. Finally, highly connected Al^{3+}-MOFs such as CAU-10 and isostructural MIL-160 have been reported to be stable in the presence of H_2O, NH_3 and H_2S [82,83].

Table 2
Possible effects of the presence of contaminants in the gas streams on the MOFs.

Contaminant	Possible effect	Ref.
Water vapor	Weakening metal-oxygen interaction	[64–66]
	Bonds undergo to phase transformation leading to a framework decomposition	[73]
	Competitive sorption with CO_2 and other gases	
NH_3	Irreversible losses in the structural porosity	[67]
	Creation of diamine-metal complex	
NH_3+H_2O	Decomposition of the MOF	[68]
	H_2 bonding between metals leading to a massive decrease in adsorption capabilities	
H_2S	Protonation of bond between metals and ligands leading to a break and framework collapsing	[69]

Many hydrolytic and gas-stable MOFs contain another critical structural feature: strongly donating ligands such as azolates, which enable stronger metal-ligand bonds. Dinca et al. reported that a series of azolate-based MOFs exhibited excellent stability to different contaminant gases [84,85]. For example, Co_2Cl_2BTDD (where BTDD is bis(1H-1,2,3-triazolato [4,5-b],[4′,5′-i])dibenzo [1,4]dioxin) was highly resistance to both water vapor and NH_3. Similarly, Navarro et al. reported a series of MOFs featuring the linker $BDP\text{-}X^{2-}$ (where $BDP\text{-}X^2$ is 1,4-benzene-dipyrazolate-2-X (X = H, OH or NH_2)) for SO_2 adsorption. Breakthrough experiments were conducted using typical complex flue gas mixtures consisting of $N_2/CO_2/SO_2$ (83.5:14:2.5) and $N_2/H_2O/SO_2$ (94.1:3.4:2.5). The presence of water vapor or CO_2 does not significantly affect the SO_2 adsorption in $1@Ba(OH)_2$ (Fig. 2), indicating that the prepared MOFs fully retained their structural integrity [86].

3.3. Mechanisms for stable MOF-structures

Stability of MOFs, especially to water vapor, may derive from structural features other than their constituent metal clusters and ligands, which can be introduced during synthesis or post-synthetically. Fig. 3 shows the factors controlling the stability of MOF in water. MOFs with improved stability either should show tolerance for hydrolysis (thermodynamic stability) or strong steric hindrance for water to cluster or approach MOF (kinetic stability) [87]. For a thermodynamically-stable MOF, its structure should show great tolerance for irreversible hydrolysis, meaning that the metal coordination sites (electron acceptor) are inert enough to resist the attack of oxygen (electron donor) from water. In this line, the metal-ligand bond strength and the lability of the metal cluster towards water controls the MOF's thermodynamic stability. As shown in Fig. 3, the metal-ligand bond strength is governed by the pKa of the coordination atom on the ligand, metal oxidation state and ionic radius. Ligands with high pKa values (such as pyrazolate ligand, pKa = 19.8) have been successfully used in the preparation of highly stable Co-, Ni, Zn- and Cu-based MOFs [88,89]. Also metals with high oxidation state, such as Fe^{3+}, Cr^{3+} and Zr^{4+} have been selected to synthesize water-resistant MOFs, for example, in UiO-type MOFs [44,74,90,91].

In addition to increasing the metal-ligand bond strength, the lability of the metal cluster toward water which are influenced by the reduction potential, Irving-Williams series of the metal and the coordination geometry of the ligand, need also to be considered. Liu et al. [72] investigated the steam conditioning effect on CO_2 adsorption capacity of DOBDC MOF/MOF-74 series and found that MOFs with less reductive metal centers are even more stable than those possessing more reductive metal centers (e. g. stability Ni/DOBDC > Mg/DOBDC). As to the kinetic stability, increasing the activation energy for hydrolysis is the primary goal to maintain the MOF structure stable under humid conditions. Commonly used methods, including the introduction of hydrophobic

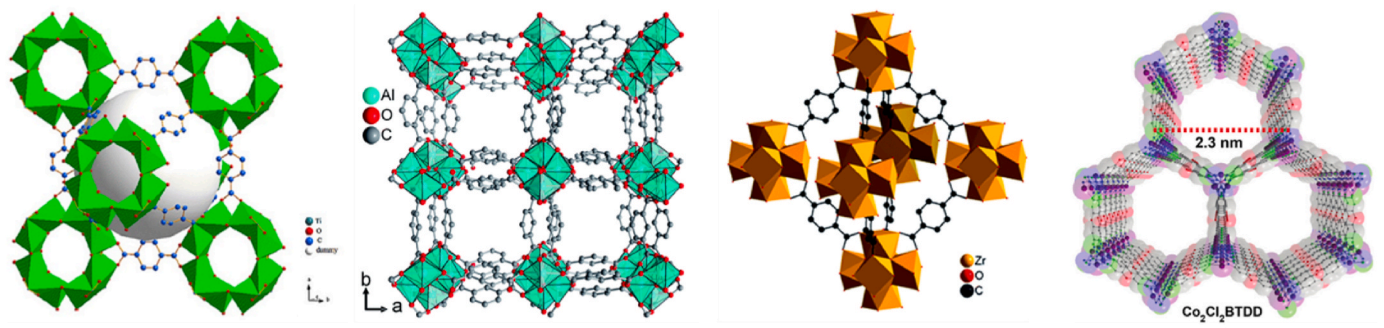

MIL-125 (Ti) CAU-10-H UiO-66 (Zr) Azolate-based MOFs

Fig. 1. Some typical stable MOF structures. Reproduced with permission from refs. 77, 79, 84, Copyright Royal Society of Chemistry and American Chemical Society.

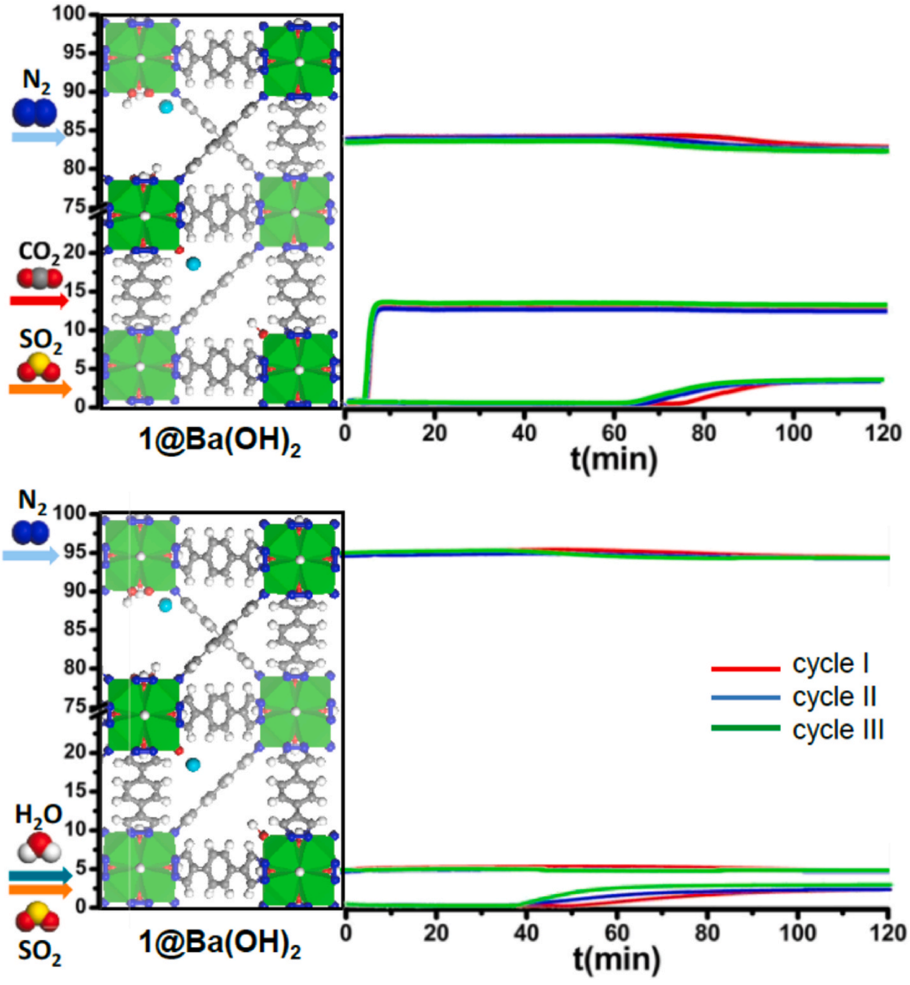

Fig. 2. Flue gas $SO_2/CO_2/N_2$ (82.5:15:2.5) breakthrough curves for 1@Ba(OH)2 at 303K showing the effect of the competitive adsorption of CO_2 on the capture of SO_2 (top). Effect of the presence of 80 % relative humidity on the SO_2 capture properties of 1@Ba(OH)$_2$ (down). Time scale normalized to 1g of MOF adsorbent. Reproduced with permission from ref. 86, Copyright 2017, Springer Nature.

groups onto the pore surface [92–94], incorporation of desired functionality at the metal node [95], and coating hydrophobic protective layer on the crystal surface [96,97], have been used to prevent the attack of water molecules to the coordination bonds to improve MOF stability.

4. Stability of MOF-based membranes

MOF membranes can generally be divided in three families. In the first one, an intergrown thin MOF layer supported by a porous support is acting as the selective layer. In the other two families, MOF particles are dispersed in a polymer matrix (MMM) and either used in a self-supported manner, or applied as a thin composite asymmetric MOF MMMs on a support. The first type of MOF membrane was reported in 2008 by growing $Cu_3(BTC)_2$ on alumina support using a seeding approach [98]. After that, Zhu et al. successfully prepared a defect-free $Cu_3(BTC)_2$ with high H_2 selectivity over other gases by means of “twin

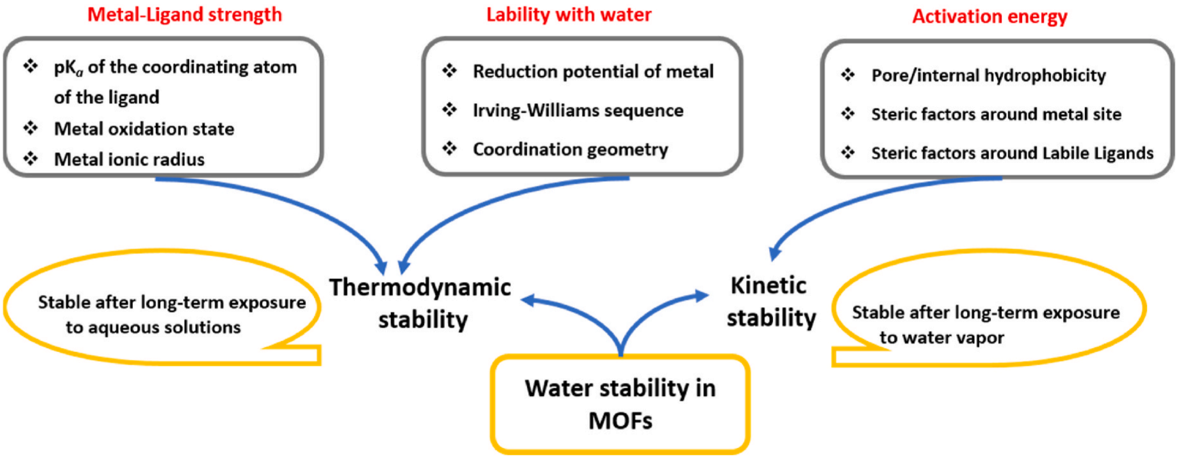

Fig. 3. Factors controlling water stability in MOFs. Reproduced from ref.87, Copyright 2014, American Chemical Society.

copper source" technique [99]. Then, different methods, such as second growth, contra-diffusion, interfacial synthesis, covalent functionalization, layer by layer growth and electrochemical synthesis were developed for preparing thin supported MOF membranes [100–108]. Despite these achievements, the synthesis of large-area, defect-free, long term-stable pure MOF membranes on a porous support remains still very challenging. In this sense, it is more convenient to prepare large-scale MOF-based MMMs without defects since only a small concentration of MOFs is required in processable polymers. Since the first research on free-standing symmetric MOF MMMs in 2004 [109], a large number of MOFs have been incorporated into polymer matrices to develop high-performance membranes [19,110,111]. Symmetric (self-standing) MOF MMMs is by far the most frequently studied class of membranes owing to the simple preparation processes. However, the symmetric MOF-based MMMs normally have a thickness of more than ~50 μm to maintain required mechanical stability, reflecting in significantly lower permeance of the membrane, and are seemingly of prime fundamental and academic interest. Considering practical industrial applications, composite asymmetric MOF-based MMMs with a thin selective MOF-polymer matrix layer on top of porous support are a potentially good trade-off between facile production at large scale and achieving high permeance [112,113]. The MOF particle size should be small enough (less than 1/3 size of the thickness of the selective layer) or use of MOF nanosheets as fillers to obtain a thin selective top layer [33,114,115]. Another important factor is the expensive cost of the synthetic MOFs. However, as only a very tiny amount of MOF is needed for the preparation of thin composite MMMs, the MOF price is in fact negligible. Recently, several reviews have summarized the progress and rational design strategies of obtaining high-performance MOF MMMs for gas separation [47,48,116]. However, only a limited number has discussed the long-term stability of MOF-based MMMs for CO_2 separation. In this sense, Table 3 summarizes most MOF-based MMMs that has undergone long-time measurements or were tested using a feed gas with relevant contaminants.

4.1. *Stability of ZIF based MMMs*

Table 3 shows that ZIF and UiO series are the most studied MOFs that have been tested for a longer duration in MMMs [26,143–145]. Li et al. [135] synthesized an amino-functionalized ZIF-7 via mixed-linker strategy and embedded them as fillers in cross-linked polyethylene oxide (XLPEO) to prepare MMMs. As shown in Fig. 4a, the CO_2 permeability was greatly improved after the incorporation of ZIF-7-NH_2. More importantly, the incorporation of ZIF-7-NH_2 interacts with the polymer matrix eliminating somehow the rubbery behavior and showing the typical behavior of a glassy polymer due to the chelating effect between the zinc nodes of the filler and the ester group of XLPEO. Only 9 % reduction in CO_2/CH_4 selectivity was observed for the MMMs up to 30 bar feed pressure, while more than 40 % reduction for the pure XLPEO membrane appeared already at 20 bar (Fig. 4a and b). In addition, the MMMs exhibited an excellent stability at 10 bar with satisfied CO_2 permeability and CO_2/CH_4 selectivity for more than 1000 h (Fig. 4c). Yang et al. [122] reported the stability of 27 wt% ZIF-8@P84 MMMs tested for CO_2/CH_4 separation at a feed pressure of 3 bar and room temperature. The membrane performance was evaluated for 720 h with constant CO_2/CH_4 selectivity and CO_2 permeability, indicating its long-term stability.

In addition to the above long-term test under dry feed conditions, Chuang's group [118] investigated the effect of CO and water vapor on the mixed H_2/CO_2 separation performance. The results demonstrated that the presence of CO in the feed stream has almost has no effect on the CO_2 permeability but leads to a slight decrease in H_2 permeability, resulting in an overall decrease of the H_2/CO_2 selectivity for the 30 wt% ZIF-8@PBI membrane. However, for the 60 wt% ZIF-8@PBI membrane, both CO_2 and H_2 permeabilities decreased (more significant for CO_2), resulting in an increased H_2/CO_2 selectivity. This is due to the competitive sorption of gas molecules and the pore blocking effect by CO. CO has the largest kinetic diameters (~3.76 Å) among these three gas mixtures, while ZIF-8 only processes a very small window aperture (~3.4 Å) for gas molecules to pass through. Thus, the presence of CO might affect both the diffusion and sorption for H_2 and CO_2, but the affectation degree varies with ZIF-8 loading in the polymer matrix.

Water vapor in the feed gas did not significantly change the membrane performance at 503 K, indicating the stable separation performance of ZIF-8@PBI membranes. However, the influence of moisture on the separation performance of ZIF-8 based MMMs may differ from each other when using different polymers or different test conditions. For example, Dai et al. [146] reported that water vapor caused a dramatic decrease of CO_2 permeability with limited effect on CO_2/N_2 selectivity of ZIF-8/PTMSP membranes upon the introduction of a small amount of water vapor (Relative humidity ≈ 25) in the feed gas mixtures at room temperature. This is an indication that the behavior of MMMs is highly depending on the type of polymer matrix used. For highly permeable polymers, as poly(1-trimethylsilyl-1-propyne) (PTMSP), the water vapor is "condensed" in the outer part of the MOF. In the other hand, for "low-permeable "or "ultralow-permeable "polymers such as polybenzimidazole (PBI), the water vapor diffuses preferentially through the MOF, which avoids condensation of water at the outer part of the MOF. This may reduce the free volume at the polymer/particle interface, and further hinder the gas transport through the membrane. However, higher operating temperatures could limit the water condensation in the membrane, and thus moisture in the feed has a negligible effect on the

Table 3

MOF- based MMMs that have been tested for longer duration or tested under feed gas with contaminant.

MMMs			Performance							Operation conditions					Ref.
MOF	Polymer	MOF loading wt %	P_{CO2}	P_{N2}	P_{H2}	P_{CH4}	$\alpha_{CO2/N2}$	$\alpha_{CO2/CH4}$	$\alpha_{H2/CO2}$	T (K)	P (Bar)	Contaminants	Testing time/h	$\alpha_{end}/\alpha_{start}$	
			(Barrer)				–								
ZIF-8	Pebax-2533	30	~750	~14	–	–	~52	–	–			100 % humidified mixed gas	29	~100 %	[117]
	PBI	30	15	–	400	–	–	–	27	503	2	1 mol. % CO	–		[118]
		60	150		2000				12						
		30	19		450				~27			1–11 mol. % H_2O	–		
		60	37		2000				14				–		
	Pebax-1657	20	290	9.4	–	–	31	–	–	298	2	–	360	~97 %	[119]
	PVA/PG	5	320	0.94	–	–	340	–	–	368	2.5	–	432	~87 %	[120]
	Polyimide	0.4	23.2		338	–	–	–	14.6	453	3	–	168	~100 %	[121]
	P84	27	11			0.12		93		298	3	–	720	~100 %	[122]
	Matrimid	20	14	–	–	2.1	–	29		308	8.5	humidified	–		[123]
PEI-ZIF-8	Pebax-1657	5	13GPU	0.26GPU	–		49	–	–	298	1	–	240	~88 %	[124]
ZIF-8-d-MK	PVAm	3	237GPU	2.49GPU	–	–	95.3	–	–	298	1	–	360	~100 %	[125]
MWCNTs@ZIF-8	Pebax®-MH-1657	8	186.3	3			61.3			308	5	–	168	~100 %	[126]
UiO-66	Matrimid	20	13			2.6		34		–	–	–			[123]
	6FDA-DAM	14	385			25.3		15.2		308	20	–	20–30		[51]
UiO-66-NH_2	PEBA	10	130	1.8	–	–	72	–	–	293	1	85 % RH	100	~103 %	[127]
	Pebax-1657	2	224	–	–	14.4	–	18.5	–	298	5	Humid	–		[128]
		1.5	267			8.6		26							
	PVAm	28.5	424	4.7	–	–	91	–	–	298	3	140 ppm SO_2, 70 ppm NO_X, 100 ppm CO 6.5 vol% O_2	80	~84 %	[129]
	PEI	18	394		33	–	–	–	12	298	1	–	100	~100 %	[130]
	6FDA-DAM	16	243	–	–	25.5	–	9.5	–	308	20	5 mol.% H2S	20–30		[51]
UiO-66-NH-$COCH_3$	6FDA-DAM	16	193	–	–	10.6		18.2	–						
UiO-66@HNT	Pebax	20	119.08	1.56			76.26			298	5		168	~100 %	[131]
ZIF-300	PEBA	30	83	0.98	–	–	84	–	–	298	4	–	100	~106 %	[132]
ZIF-301	6FDA DAM	20	891			30.4		29.3		298	4		120	~100 %	[133]
ZIF-302	P84	30	5.5	0.11			50			333	3	30 % RH	33	~100 %	[134]
ZIF-7-NH2(70)	XLPEO	30	200	–	–	4	–	50	–	308	10	–	1000	~98 %	[135]
MOF-801	PEBA	7.5	29.1	–	–	–	66	–	–	293	1	–	120	~97 %	[136]
	PIM	5	9686 ± 799	362 ± 40			27 ± 1.6						120	~107 %	[137]
Y-fum-fcu-MOF	6FDA-DAM	13	475	–	–	–	–	43.9[a]		308	6.7	20 % H_2S	–		[110]
CuBTC-ns	PIM-1	10	267	–	–	17-	–	15.6	–	298	1	–	100	~88 %	[114]
Cu-BTC-SC	Pebax® 1657	15	~1102.5/ 1069.6GPU	20.12GPU		32.91GPU	54.8	32.5		298	1.5	H_2O	100	~80 %	[138]
Gly@CuBTC	Pebax MH 1657	5	175			6.03		29				humidified	100	~88 %	[139]
MFU-4	6FDA–Durene	10	1180 (H2S + CO2)			28		42.0[a]		308	2	20/20/60$H_2S/CO_2/CH_4$			[140]
(001)-AlFFIVE	6FDA-DAM-DAT	59.6	358.6 305.5					135.6[a] 143.7[a]		308	10	1/9/90$H_2S/CO_2/CH_4$ 5/5/90$H_2S/CO_2/CH_4$	720	~100 %	[141]
PVAm Modified MIL-101(Cr)	PVAm	44.44	823GPU	3.4GPU			242			298	5	14.2 % CO_2, 6.5 % O_2, 120 ppm SO_2, 80 ppm NOx, 10 ppm CO, and balanced with N_2	150	~100 %	[142]

[a] $\alpha_{CO2+H2S/CH4}$.

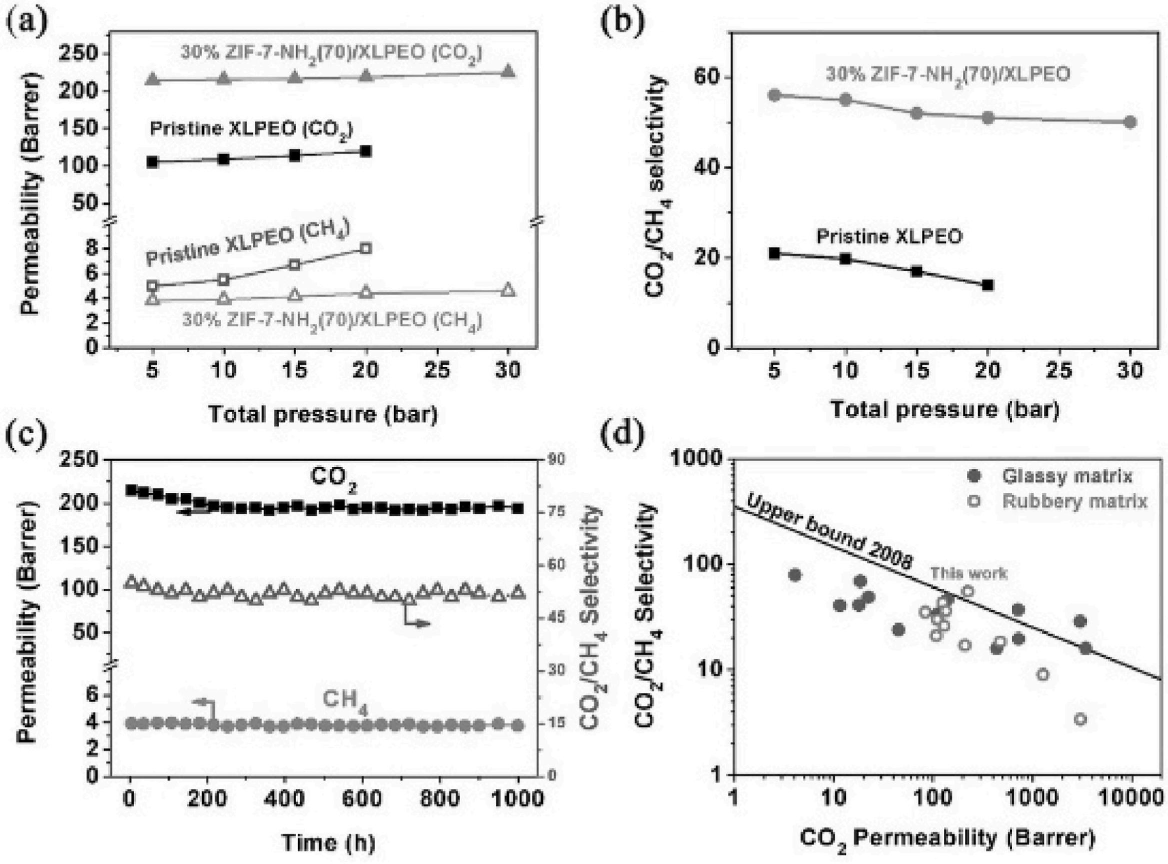

Fig. 4. (a) Permeability and b) separation factor of equimolar CO_2/CH_4 mixed-gas on the pristine XLPEO membrane and 30 % ZIF-7-NH2(70)/XLPEO MMMs, c) long-term stability for CO_2/CH_4 separation on 30 % ZIF-7-NH_2(70)/XLPEO MMMs at 10 bar and 35 °C, d) comparison of CO_2/CH_4 separation performance with previously reported MMMs from both glassy and rubbery matrices. Reproduced with permission from ref. 135, Copyright 2017, Wiley-VCH.

separation performance of some ZIF-8 based MMMs tested at elevated temperatures.

4.2. Stability of UiO- based MMMs

Compared to ZIF-8 based MMMs, UiO-66 based MMMs are more stable under humid conditions. The Jin group [127] reported the effect of humidity on the separation performance of UiO-66-NH_2-PEBA MMMs towards CO_2/N_2. The CO_2 permeability significantly increased with slightly enhanced CO_2/N_2 selectivity after humidifying. This is due to the facilitated CO_2 transport in the membranes triggered by water vapor, arising from the hydrophilic as well as CO_2-philic properties of UiO-66-NH_2. More excitingly, the 10 wt% UiO-66-NH_2-PEBA membrane exhibited high and stable performance with an average CO_2 permeability of 130 Barrer and a CO_2/N_2 selectivity of 72 during 100 h with 85 % relative humidity in the feed gas.

Wang et al. [129] utilized a 'bridging-cross-linking' method to connect poly(vinylamine) (PVAm) and UiO-66-NH_2 nanoparticles via poly (ethylene glycol) diglycidyl ether (PEGDE) (the abbreviation of this mixture is BUPP) and then coated the BUPP solution on modified polysulfone (mPSU) substrates. The prepared composite BUPP/mPSU membrane (28.5 wt% UiO-66-NH_2) achieved a high CO_2 permeance of 531 Barrer together with a CO_2/N_2 selectivity of 91 at 3 bar under dry feed conditions. Importantly, Wang et al. [129] first tested MOF MMMs under practical industrial flue gas mixtures containing SO_2, NOx, CO and O_2 as well as large amount of CO_2 and N_2. As shown in Fig. 5, the BUPP/mPSU membrane (28.5 wt% UiO-66-NH_2) was first treated with CO_2/N_2 (v/v 15/85) for 8 h and then evaluated under a synthetic feed gas mixture (14.5 vol% CO_2, 6.5 vol% O_2, 140 ppm SO_2, 70 ppm NOx, 10 ppm CO and balanced by N_2) for 80 h. The CO_2 permeability and CO_2/N_2 selectivity of the BUPP/membrane decreased by 19.5 and 16.5 %, respectively, when the feed gas changed from a CO_2/N_2 (v/v 15/85) mixture to a simulated flue gas. The separation performance remained stable under simulated flue gas and could retrieve the initial performance when switched the feed gas to CO_2/N_2 mixture.

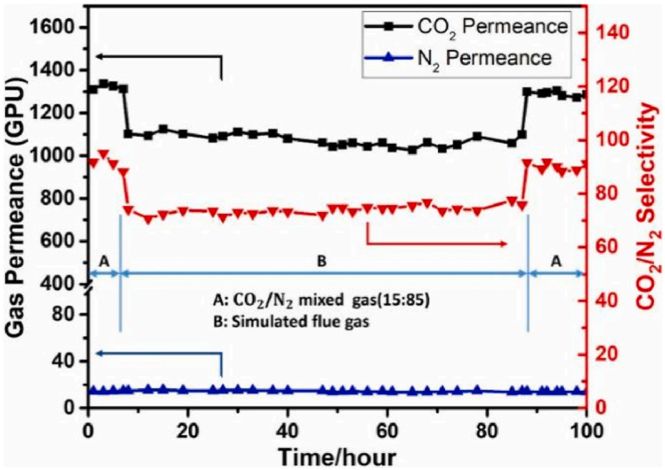

Fig. 5. The stability test of the BUPP/mPSU membrane. Feed gas: CO_2/N_2 (15/85) mixed gas and simulated flue gas (14.5 vol% CO_2, 6.5 vol% O_2, 140 ppm SO_2, 70 ppm NOx, 10 ppm CO and balanced by N_2). Feed gas pressure: 3 bar. Reproduced with permission from ref. 129, Copyright 2019, Elsevier.

4.3. Stability of other MOF based MMMs

Both CO_2 and H_2S, present as typical impurities in natural gas, must be removed from CH_4. The removal performance can be evaluated by testing the total acid gas permeability [$P(CO_2) + P(H_2S)$] and selectivity [$P(CO_2) + P(H_2S)]/P(CH_4)$] [110,140,141]. In 2018, Eddaoudi et al. [110] prepared a 13 wt% Y-fum-fcu-MOF/6FDA-DAM hybrid membrane for the separation of 20/20/60$H_2S/CO_2/CH_4$ mixtures. Likely, the resultant composite membranes exhibited a $(CO_2{+}H_2S)/CH_4$ selectivity of 43.9 and a high permeability of 475 Barrer for total acid gases. Recently, their research group developed an acid-stable MOF-based MMM composed by in-plane aligned (001)-AlFFIVE-1-Ni nanosheets and 6FDA-DAM-DAT matrix. The prepared MMMs were tested under realistic raw natural gas composition ($H_2S/CO_2/CH_4$: 1/9/90; 5/5/90). As shown in Fig. 6, under each $H_2S/CO_2/CH_4$ mixture, both the mixed gas ($H_2S + CO_2$) permeability and the $(H_2S + CO_2)/CH_4$ selectivity were relatively constant for at least 30 days of continuous testing at 10 bar and 35 °C [141]. Smith et al. [140] synthesized an MMM system made from a 6FDA−Durene polymer and an MFU-4 MOF, for which the mixed $(H_2S + CO_2)/CH_4$ permselectivity could reach to 42 together with high CO_2 and H_2S permeability. The above studies demonstrated that MOF-based MMMs can reach exceptionally performance and long-term stability for carbon dioxide separation from natural gas.

4.4. Perspective for future MOF-based MMM stability studies

In a broader view, the results in Table 3 also demonstrate that stability of MOF-based MMMs is insufficiently studied to warrant success in industrial application. Most studies test the membrane stability for approximately 100 h. Only three studies were found that tested for more than 500 h, and none of the stability studies was prolonging for over 1000 h (which is just over a month). At the same time, industrial deployment requires stability for years. Hence, either longer stability tests or accelerated stress tests are required to prepare MOF-based MMM for practical applications.

Regarding the type of contaminations, humidity is best studied for several MOF types. Also sulphur-based contaminants have been studied for several MOF-based MMMs, with mixed results. However, other acidic and basic contaminants, such as HCl and NH_3, are poorly studied for any of the MOF-based MMMs. At the same time, it is known that acid gases and NH_3 can cause MOF degradation (Table 2). MOF-based MMMs are available for NH_3/N_2 or NH_3/H_2 separation [147], which offers perspective for also making NH_3-stable MOF-based MMMs for CO_2 separation. Introducing functional groups containing Lewis acid site (carboxyl-, sulfonic-, hydroxyl-) into MOFs enable the prepared MMMs absorb ammonia basic gas from CO_2 gas mixture and at the meantime increase the solubility coefficient towards CO_2 through the chemical interaction between these polar groups and CO_2, thus obtaining excellent gas separation performance.

Apart from long-term stability under contaminate gases, it is essential to pay attention to the anti-aging and plasticizing characteristics of MMMs used for gas separation. The physical aging process of membranes can result in a reduction in gas permeability while a slight increase in selectivity especially for high fraction free volume polymers, which is unfavourable for industrial applications [148–150]. Introducing MOFs in polymer matrix can usually improve the anti-aging of polymer membranes through good interface interaction. For example, Qiao et al. [151] incorporated defective UiO-66-FA into the PIM-1 matrix and enhanced the interfacial compatibility by forming a hydrogen bond network. The gas permeability of the MMMs only decreased by 25 % after 160 days of continuous operation. This improvement can be attributed to the incorporation of MOF nanoparticles acted as supports which effectively prevents the pore collapse in PIM-1 membrane, consequently mitigating its aging process. In contrast to aging, membrane plasticization causes the permeable components to swell through the membrane, resulting in reduced selectivity for gas separation. Currently, loading MOFs into polymer membranes is an effective approach to improve their resistance to plasticization [150,152]. For instance, Ahmad et al. [153] added Zr-MOFs nanoparticles into 6FDA-DAM polyimide to fabricate MMMs and investigated their plasticization behavior in the CO_2/CH_4 separation system. The study revealed that as the pressure increased to 20 bar, the CO_2 permeability coefficient and CO_2/CH_4 separation factor exhibited a decrease trend. Overall, MOF fillers can usually effectively inhibit the aging and plasticization of polymer membranes by restricting the polymer chain mobility through good interface interaction [151–153].

5. Scalable synthesis of MOFs and MOF-based MMMs

5.1. Scalable synthesis of MOFs

MOFs are lauded for their potential in diverse industrial applications such CO_2 capture. However, the progress of MOFs into the commercial sphere remains limited by several factors, including the scale-up of laboratory syntheses to pilot production [154]. Among processes explored for production of MOFs, solvothermal batch synthesis was the first to enable production of MOFs above laboratory scale. Solvothermal synthesis involves the use of sealed reactors in which a solvent is heated

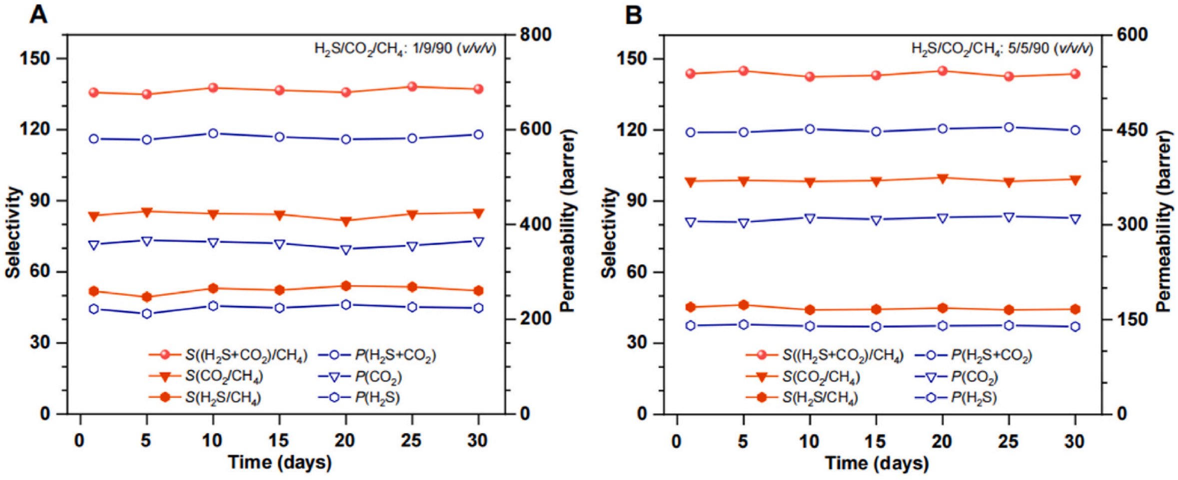

Fig. 6. (A and B) Membrane stability under different H_2S concentration, (A) $H_2S/CO_2/CH_4$: 1/9/90; (B) $H_2S/CO_2/CH_4$:5/5/90. Robust $H_2S/CO_2/CH_4$ separation properties of (001)-AlFFIVE(59.6)/6FDA-DAM-DAT membrane for at least 30 days. Feed pressure at 10 bar and 35 °C. Reproduced with permission from ref. 141, Copyright 2022, Science.

to temperatures above the boiling point of all solvents, to dissolve the reagents (inorganic salts and organic linkers) and favor their reaction to form the target MOF. Using this approach, Wang et al. prepared 80 g of HKUST-1 [155] and Stock and Biswas prepared 50 g of MOF-5 [156]. Similarly, Seo et al. synthesized Mg-MOF, and Czaja, Trukhan and Müller synthesized MIL-100(Fe), both at the kilogram scale, obtaining space-time yields (STY) of 300 kg/m^3·day and 1700 kg/m^3·day, respectively [157,158].

Although the solvothermal batch method is common in industry, it suffers from certain drawbacks. For example, heating of large reaction vessels is energy intensive. Moreover, since crystallization of MOFs occurs preferentially at vessel surfaces, and increasing the size of a reactor vessel decreases its surface-to-volume ratio, increasing the scale of MOF production leads to a diminishing number of nucleation sites. This scaling problem can be mitigated using microwave irradiation. Microwaves acts as high-frequency electric fields, causing any materials that have electric charges (*e.g.* ions or polar molecules) to move and consequently, to heat up. The thermal energy generated inside a microwaved solution can be transformed into chemical energy for endothermic reactions. Thus, while in classical solvothermal reactions, MOFs preferentially crystallize on the vessel wall, in microwave-assisted solvothermal reactions, MOFs begin to crystallize in solution. Accordingly, microwave-assisted solvothermal synthesis tends to be faster and more efficient than the traditional method. It also tends to produce smaller crystals in comparison to standard solvothermal reactions, which is desirable for MMM for which MOF crystals must be incorporated into defect-free films. Using this methodology, Jhunget and coworkers first prepared MIL-100(Cr) [159]. Since then, numerous reports of microwave-assisted MOF syntheses have revealed that MOF particle-size, crystallinity and morphology can all be controlled by modulating the irradiation time, reagent concentration, temperature or substrate composition [160–162]. For example, Férey et al. optimized the crystallinity of MIL-100(Cr) and controlled the particle size (from 40 nm to 200 nm) by increasing the irradiation time. Alternatively, Masel et al. and Ahn et al. each demonstrated that, by increasing the temperature, power level and reagent concentrations, they could accelerate the synthesis of IRMOFs, albeit with a concomitant loss in crystal quality. Recently, Cao et al. reported the gram-scale production of nine microporous lanthanide MOFs *via* microwave synthesis [163], and Taddei and co-workers described an optimized microwave-assisted production of UiO-66 (particle size: 300 nm), with an excellent STY of 2241 kg/m^3·day [164].

For industrial production of MOFs, in parallel to batch synthesis, several methods for continuous production have been developed [165,166]. One example is flow chemistry, whereby reactions occur in a continuously flowing stream characterized by a higher surface-to-volume ratio than in traditional reaction vessels, thus providing superior heat transfer than in batch syntheses of comparable scale. Moreover, compared to batch synthesis, flow chemistry synthesis can be readily scaled-up, as the reaction parameters can be precisely controlled and the reactors, easily scaled-up. Thus, given its lower energy consumption, and its lower demands for solvent volume, flow chemistry tends to be more cost-effective and environmentally friendly than batch synthesis. There are various flow-reaction systems, including microfluidic reactors, plug-flow reactors and stirred-tank reactors. Ameloot et al. pioneered the use of microfluidic reactors to synthesize MOFs. For instance, using a biphasic reaction mixture comprising two immiscible solvents, each of which contained one of the two components of HKUST-1, they induced HKUST-1 crystallization in a liquid–liquid interface, obtaining homogeneous HKUST-1 membranes [167]. Unfortunately, this methodology is limited to lab scale, as scale-up would require large volumetric reactors. An alternative to microfluidic reactors is a plug-flow reactor, in which solutions of the precursors are introduced separately into a tube reactor, flowed through it and then, reacted. This method was first used by Gimeno-Fabre et al. to synthesize HKUST-1 (particle size: 10 μm) and Ni-CPO-27 (particle size: 20 nm) [168]. Using the same system, Mann and co-workers later synthesized ZIF-8 at the kilogram scale, obtaining an STY of 11,625 kg/m^3·day [169]. Remarkably, Rubio-Martínez et al. reported the efficient synthesis of a series of MOFs using a pilot plug-flow reactor (volume: 1394 L), including Al-Fum (particle size: 200 nm) at an STY of 97,159 kg/m^3·day [170]. Finally, in stirred-tank reactors, which marry batch synthesis to continuous flow, the reagents are continuously introduced into a heated, stirred reactor vessel. As the reagents are gradually added, the newly-formed MOFs are continuously recovered from the vessel to regenerate the reaction medium. This method was firstly used by Schoeneker et al. to synthesize 10 g of UiO-66-NH$_2$ in a 2-L flow crystallization reactor [171]. Using a similar approach, McKinstry et al. improved the synthesis of MOF-5, obtaining an STY of 1000 kg/m^3·day.

Using this same strategy of continuous flow reactors, MOF synthesis can be performed in microwave-assisted flow chemistry, which in some cases has provided markedly higher STY values than in the corresponding microwave-assisted batch reactions. For instance, Ranocchiari, Taddei and co-workers reported the continuous-flow, microwave-assisted synthesis of UiO-66, MIL-53(Al) and HKUST-1 with STY values of 7204 kg/m^3·day, 3618 kg/m^3·day and 64,800 kg/m^3·day, respectively [172]. Likewise, Stock et al. produced Zr-fum at an STY of 2733 kg/m^3·day [173]. More recently, the groups of McKinstry and of Laybourn synthesized HKUST-1 (size: 100 nm) at STY values of 632,000 kg/m^3·day, using a continuous-flow oscillatory baffled reactor equipped with a homogeneous, controllable microwave [174]. In 2013, Carné-Sánchez et al. reported [174] a new approach, known as spray-drying, which entails the atomization of a solution of MOF precursors into a spray of microdroplets, using a nozzle. This is accomplished by simultaneously injecting the solution and compressed air or nitrogen gas into a reaction chamber. Next, the atomized microdroplets are heated by the injected gas, causing the solvent to evaporate which induces the formation of MOF nanocrystals. Full evaporation of the solvents leads to formation of MOF nanocrystals, which in turn assemble into spherical compact or hollow MOF beads. Note that the MOF-precursor solution can be injected using a two-fluid nozzle, a three-fluid nozzle or a T-junction. Also, this solution can be pre-heated before injection, using a flow reactor. To date, myriad MOF beads (*e.g.* HKUST-1, MOF-74 family, ZIF-8, UiO-66 and CuBDC) have been synthesized by spray-drying. In some cases, the resultant MOF beads can be mechanically disassembled into MOF nanocrystals, which can then be isolated. This has been reported for isolation of nanoparticulate HKUST-1 (Fig. 7, size: 75 nm), UiO-66 (size: 30 nm), ZIF-8 (size: 50 nm), MOF-74(Ni) (size: 130 nm) and NOTT-100 (size: 60 nm) [175]. Recently, Avci-Camur et al. explored the use of water as solvent in spray-drying synthesis of MOFs such as UiO-66 MOFs and HKUST-1 [176]. For instance, using this technique at a pilot spray-drying plant, they produced 60 kg of HKUST-1.

Finally, another valuable method for large-scale production of MOFs is mechano-synthesis, whereby (typically) solid reagents are mechanically reacted to form diverse molecular or supramolecular compounds. This enables solvent-free chemistry, or at least, use of only minimal volumes of solvent. The mechanical energy that underpins the reactions is typically generated by grinding a physical mixture of two solid reagents in a mortar, ball-mill or extruder. This approach allows for use of MOF precursors with poor solubility (in water or organic solvents), including carbonates, hydroxides and oxides. Accordingly, compared to other methods for industrial MOF production, mechano-synthesis can be considered faster, more environmentally friendly and more efficient, as it often affords MOFs in quantitative yields. Representative mechano-syntheses of crystalline structures include work by James et al., who recently prepared HKUST-1 and Cu(INA)$_2$ this way [177]. Mechano-syntheses have been scaled-up via *extrusion*, a continuous process that involves the movement of material along a set of screws. James et al. reported synthesis of Al-Fum and of HKUST-1 with twin-screw extrusion, and of ZIF-8 in single-screw extrusion, obtaining STY values of 27,000 kg/m^3·day (Al-Fum), 144,000 kg/m^3·day

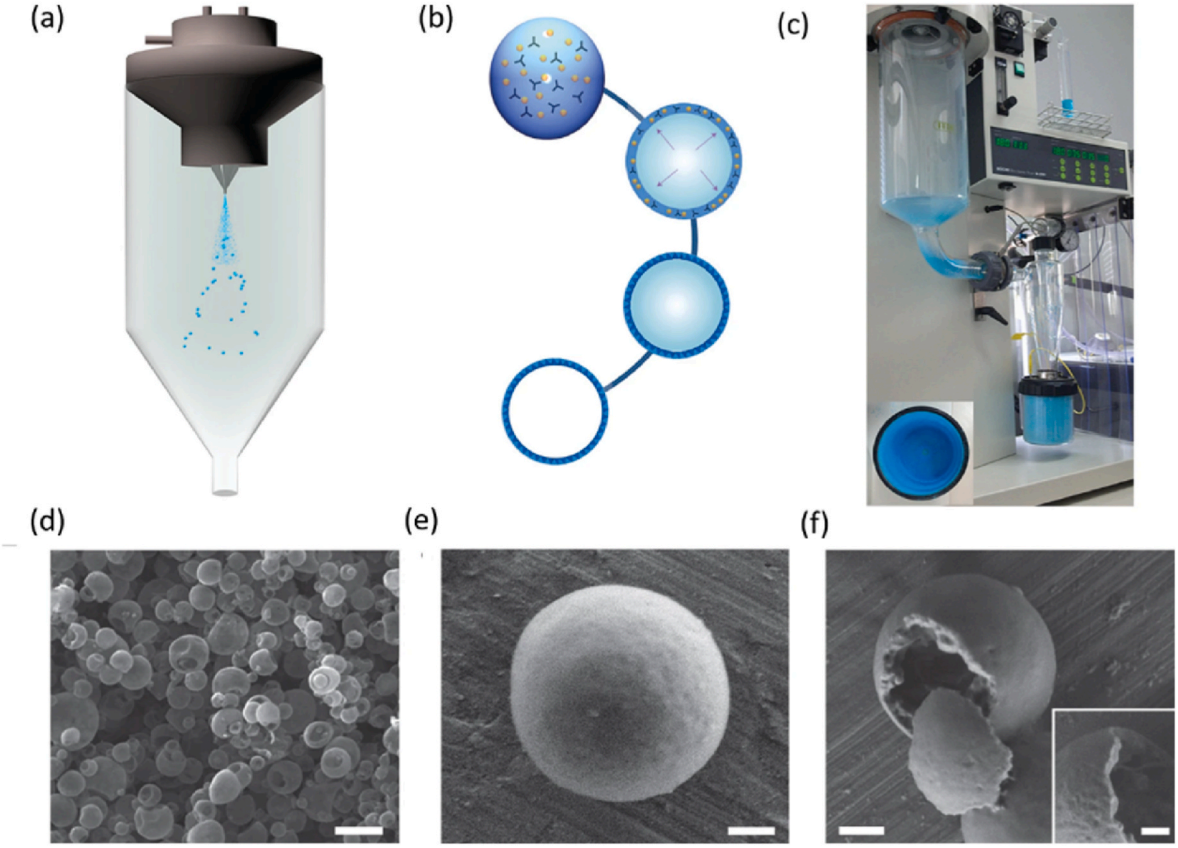

Fig. 7. (a) Schematic showing the spray-drying process used to synthesize HKUST-1 superstructures. Blue dots, sprayed solution; blue spheres, formed spherical superstructures. (b) Proposed spherical superstructure formation process (emphasized by purple arrows), which implies the crystallization of nanoMOF crystals. (c) Photograph of the spray-dryer after its use in synthesizing large amounts of blue HKUST-1 superstructures. d–f, Representative FESEM images showing a general view of the spherical HKUST-1 superstructures (d), the wall of a single HKUST-1 superstructure showing the assembly of nanoHKUST-1 crystals (e), and a mechanically broken hollow superstructure showing the internal cavity and the thickness of its wall (f and inset). Scale bars: 5 μm (d), 500 nm (e, f), and 200 nm (f inset). Reproduced with permission from ref. 175, Copyright 2013, Springer Nature. (For interpretation of the references to colour in this figure legend, the reader is referred to the Web version of this article.)

(HKUST-1) and 144,000 kg/m^3·day (ZIF-8) [178]. Similarly, Karak et al. recently applied twin-screw extrusion to large-scale synthesis of COFs, reaching production rates of several kg/h [179]. Finally, the company MOF Technologies has been exploring mechano-chemical synthesis of various MOFs, having demonstrated rapid syntheses on the multi-kilogram scale. Table 4 summarize the different methods used for scale-up synthesis of different MOFs.

5.2. Scalable synthesis of MOF-based MMMs

A number of MOF-based membranes developed at lab-scale are showing promising performances suitable for industrial applications. Although multiple examples of scalable synthesis of MOF membranes have been reported [190–192], the large scale production of defect-free MOF-based membranes is still a great challenge and commercial MOF membranes are still rarely seen. The main barriers are polymer-filler incompatibility, plasticization, MOF agglomeration or unstable MOF-polymer suspensions, leading to the formation of interfacial defects and irregular distribution of the in inorganic materials along the membrane [193–195]. Also, the required adaptation of the current membrane production processes to be able to incorporate MOF on large scale plays a significant role.

Scaling MOF-based mixed matrix membranes is strongly tied with the membrane structure and membrane module type. Most commercially available gas separation membranes are fabricated via a phase inversion process in a single step forming an asymmetric structure, or via a coating/interfacial polymerization (IP) process in one or multiple steps creating a Thin Film Composite (TFC). The shape of the membrane, and thereby also the manufacturing methods, depends on the membrane module. For gas separation applications commonly two membrane geometries are used: flat sheet and hollow fibers [196–198] (see Fig. 8). For both membrane geometries, MOF-based membranes fabrication is regular reported literature.

Table 5 lists previous work of MOF-based TFC membranes for CO_2 separation. In general, both flat sheet membranes and hollow fiber modules are able to manufacture MOF-based MMM at cm^2-scale with reasonable selectivities. While flat sheet membranes require less advanced equipment to manufacture defect-free layers, hollow fiber modules benefit from their large surface to volume ratio when scaling to larger modules [195]. Nevertheless, very few research data has been reported for MOF-based MMM at substantial scale. From Table 5, the largest scale unit (340 cm^2) that was assessed for CO_2 permeance was a hollow fiber module with ZIF-8 particles deposited by gel-vapor deposition [199]. The ultrathin layer (<100 nm) allowed to achieve an extremely high permeance.

Sasikumar et al. [205] reported a single step fabrication of a polysulfone (PSf) hollow fiber MOF membrane. The ZIF-8, SiO_2/ZIF-8, and amine-modified SiO_2/ZIF-8 were dispersed into the polymer dope solution and subsequently the hollow fiber MMM was synthesized via the phase inversion technique. Their research found, besides improved membrane performance, excellent scalability of the MOF membrane process which can be easily further developed into membrane prototypes and membrane modules for effective CO_2 separation.

Scalable synthesis of hollow fiber MOF TFC membranes was reported

Table 4
Scale-up synthesis of different MOFs using different methods.

MOF	Technique	STY (kg/ m3·day)	Reference
HKUST-1	Extrusion mechano-chemical	144,000	[178]
ZIF-8	Extrusion mechano-chemical	144,000	[178]
Al-Fum	Extrusion mechano-chemical	27,000	[178]
ZIF-8	Flow chemistry (MR)	210,000	[180, 181]
Al-Fum	Flow chemistry (PFR)	97,159	[170]
HKUST-1	Flow chemistry (PFR)	64,800	[172]
MOF-5	Flow chemistry (CSTR)	1000	[182]
UiO-66	Spray-drying	19.6	[183]
$MgFe_2O_4$@UiO-66-NH_2	Flow chemistry	300	[184]
CUP-1	Flow chemistry (MR)	550	[185]
CUP-1	Hydrothermal	20	[185]
MOF-801	Flow chemistry (MR)	367.2	[186]
HKUST-1	Flow chemistry (microwave, continuous flow, oscillatory baffled reactor)	632,000	[174]
HKUST-1	Flow chemistry (microwave, continuous flow, oscillatory baffled reactor)	400,000	[187]
MOF-74-Ni	Continuous-flow microwave reactor	720	[188]
UiO-66	Continuous-flow microwave reactor	7204	[172]
MIL-53(Al)	Continuous-flow microwave synthesis	3618	[172]
Al-Fum	Hydrothermal	3600	[189]

Abbreviations: Fum: Fumarate; MR: Microfluidic reactor; PFR: Plugged-flow reactor; CSTR: Continuous-stirred tank reactor; STY: Space-Time Yield.

by Sutrisna et al. [202], incorporating various UiO-66, and ZIF-7 MOF types into a thin PEBAX selective layer on a PVDF support with gutter layer (Fig. 9). Simultaneously improvement of the CO_2 permeance and selectivity was observed. A similar approach was reported by Li et al. [203]. Incorporating amine functionalized UiO-66 nanoparticles into the Pebax® 2533 thin selective layer on a polypropylene (PP) hollow fiber supports via dip coating process. They observed that the surface morphology of the prepared membranes was influenced by the incorporation of UiO-66 nanoparticles. The CO_2 permeance increased along with an increase of UiO-66 nanoparticles content, while the CO_2/N_2 ideal gas selectively firstly increased whereafter a decrease was observed due to the aggregation of UiO-66 nanoparticles.

Literature often indicates that a multistep coating approach is required. An intermediate gutter layer is generally based on a polydimethylsiloxane (PDMS) coating to cover up the surface defect is added to the membrane formation process [206]. Additionally, since, very thin selective layers are needed (30–100 nm) to achieve high permeance, the size of the MOFs particles is crucial in order to obtain defect-free membranes. The dual layer formation has been also tested for MMMs where again [33,117,207,208], depending on the particle content, the presence of defects is often detected. For more details on the hollow fiber MMM manufacturing process, we refer to previous review work [190].

The multiple layer coating process can be merged in a single step approach, denominated dual layer membrane formation [209]. The process has to be optimized for the particular polymeric systems in order to have a better control of the adhesion of the phases [210,211]. Dai et al. [204] reported the production of asymmetric dual layer hollow fiber membranes containing MOF ZIF-8 fillers in a polyetherimide skin layer via the dry jet-wet quench method. Enhanced permselectivity of 20 % over pure polymer was found. Although the performance was limited by the relatively low permeability of the polyetherimide. Additionally, when the solution containing the MOF is only in the outer layer, the cost of the process significantly drops since the amount of the inorganic filler used is very small.

A different approach was reported by Echaide-Górriz et al. [212] synthesizing a bilayered polyamide-MOF membrane on a hollow fiber support for application in nanofiltration. The continuous MOF layer was crystallized by liquid phase crystal growth, whereafter a polyamide layer was added on the top of the MOF via interfacial polymerization.

For scalable flat sheet membranes, Lan et al. [213] recently used an in-situ heat-assisted solvent-evaporation method to massively produce MOF-based MMMs rapidly. Importantly, this method was applicable to different polymers and MOF types. Using this method, they can obtain MMMs at industrial standards with 4 m of membrane roll in a batch

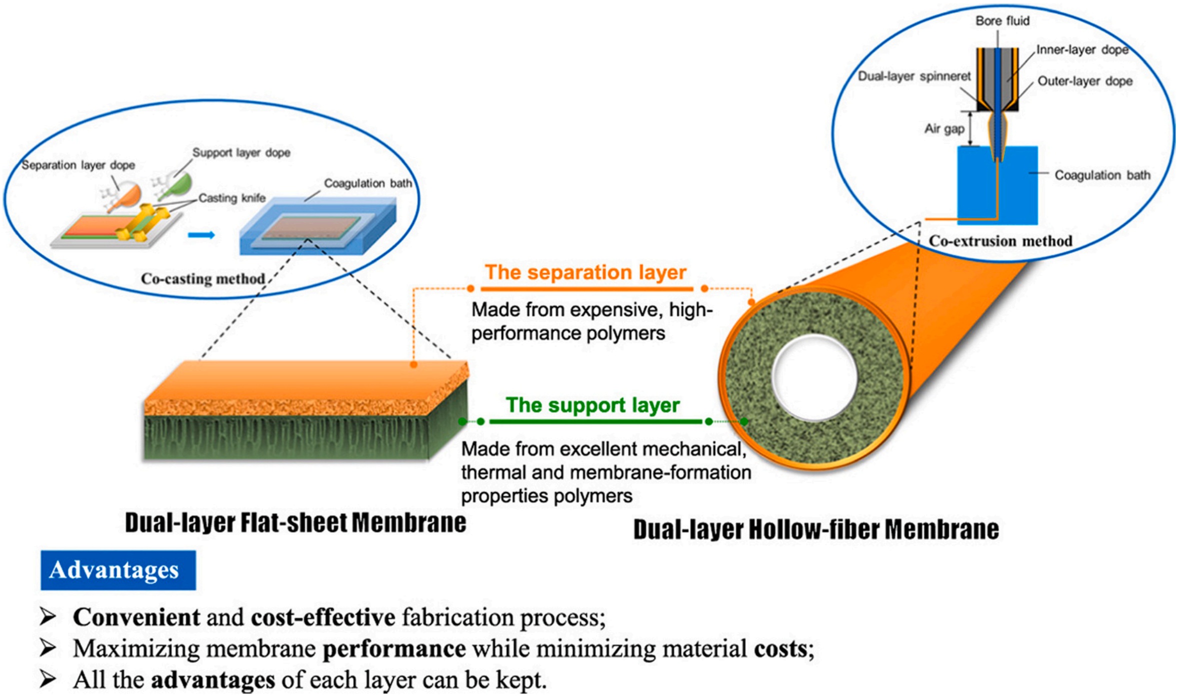

Fig. 8. Conceptual schematic of dual-layer flat-sheet and hollow fiber membranes and fabrication methods. Reprinted with permission from Ref.196, Copyright 2018, Elsevier.

Table 5
MOF-based MMM with reported area and CO_2 permeance. Data was collected for research that operated between 25 and 35 °C Selectivity is either measured from mixed gas or from the ratio in pure gas permeance.

Composition selective layer	Module type	Scale (cm^2)	Type separation	Selectivity	CO_2 Permeance (GPU)	Reference
PVA/PG/ZIF-8	Flat sheet	8.5	CO_2/N_2	370	82	[120]
PEI/ZIF-8	Flat sheet	1.1	CO_2/N_2	49	13	[124]
PVAm/ZIF-8	Flat sheet	12.6	CO_2/N_2	86.7	169	[125]
PVAm/UiO-66	Flat sheet	19.3	CO_2/N_2	91	1295	[129]
PI/MIL-53	Flat sheet	2.2	CO_2/N_2	23	20	[200]
PI/MIL-53	Flat sheet	2.2	CO_2/CH_4	23	20	[200]
PEBAX/CuBTC	Flat sheet	20	CO_2/N_2	54.8	1103	[138]
PEBAX/CuBTC	Flat sheet	20	CO_2/CH_4	32.5	1070	[138]
PI/Cu3(BTC)2	Hollow-fiber	1.1	CO_2/N_2	5.9	65	[201]
PI/Cu3(BTC)2	Hollow-fiber	1.1	CO_2/CH_4	7.7	65	[201]
PEBAX/ZIF-8	Hollow-fiber	17	CO_2/N_2	30	290	[119]
PEBAX/UiO-66-NH_2	Hollow-fiber	17	CO_2/N_2	57	338	[202]
PEBAX/UiO-66-NH_2	Hollow-fiber	8.2	CO_2/N_2	37	26	[203]
Ultem/ZIF-8	Hollow-fiber	10.5	CO_2/N_2	36	26	[204]
PSF/ZIF-8	Hollow-fiber	340	CO_2/N_2	7.3	11529	[199]
PSF/ZIF-8	Hollow-fiber	340	CO_2/CH_4	8.9	11529	[199]
PSF/ZIF-8	Hollow-fiber	340	CO_2/C_3H_8	1030	11529	[199]

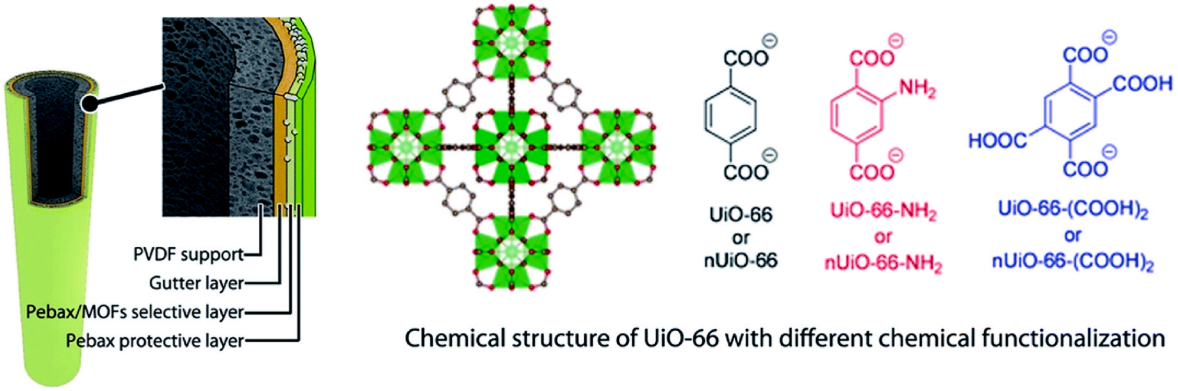

Fig. 9. Schematic diagram of the composite membrane and the chemical structure of UiO-66, for the application in hollow fiber for CO_2 separation. Reprinted with permission from Ref.202, Copyright 2018, RSC.

experiment. These MMMs demonstrated excellent mechanical strength and great performance for dye separation (Fig. 7), and they could also be readily assembled as separator in Li–S battery. Since MOF-based MMMs for CO_2 separation have been widely studied, future studies should be focused on using this powerful method for massively produce other MOF-based MMMs for CO_2 capture. Another impressive method for processing MOFs into polymer is using MOF-loaded porous liquids. Recently, Gascon et al. [214,215] used *N*-heterocyclic carbenes (NHCs) to modify the outer surface of ZIFs to make them solution processable. The NHC-functionalized ZIFs were able to form stable colloidal solutions in nonpolar organic solvents, which could then be easily co-processed with many polymers to yield high loaded MOF-based MMMs. With this method, it is expected to be able to fabricate MOF-based MMMs in large-scale considering its solution-processability.

6. Emerging COF membranes for CO_2 separation

6.1. COF based MMMs

Given the challenges in stability of MOF-based MMMs, alternative materials that can still exhibit the supreme size selectivity of crystalline MOF structures are interesting to study. Because the instability of MOF-based structures is often originating from the metal atom, either by the oxidation state or interaction with the organic structure (see Fig. 3), eliminating the metal site provides potential route for more intrinsically stable structures. This is represented in the concept of covalent organic frameworks (COFs).

COFs are a relatively new class of crystalline porous materials that are analogous to MOFs but made exclusively of organic linkers [216]. Compared to the inorganic-organic hybrid nature of MOFs materials, the pure organic nature of COFs could result in better compatibility with polymers, reducing the possibility of forming defects at the interface between polymer and filler when preparing MMMs. This compatibility was demonstrated by Banerjee et al. [18], who has successfully dispersed two chemical-stable isorectiular COFs (TpPa-1 and TpBD) in PBI-Bul to prepare MMMs with a COF loading as high as 50 %. For comparison, it is very difficult for most MOFs to reach similar loading in a polymer matrix.

The first generation of boronate-linked COFs were found unstable in presence of water, acids and alcohols [217]. This is because the electron-deficient boron sites are susceptible to be attacked by nucleophiles such as water. Therefore, even a slight amount of water vapor present in air could potentially induce the decomposition of boronate-linked COFs. Although a post-synthetic modification of the COF framework by pyridine or alkyl has been evaluated to improve the structural stability [218–220], such boron-containing COFs have still not shown the required stability for real applications. Later, hydrone-, azine-, triazine- and imine-linked COFs were successfully synthesized, demonstrating enhanced stability in neutral water, but still hydrolysis under acid conditions [221,222]. In these COFs, the introduction of special functional groups in their organic components, creating hydrogen bonding in intramolecular or interlayers, has proved helpful to further enhance their stability. For example, a robust and stable azine-linked COF, COF-JLU3, was made by forming intramolecular

O–H⋯N═C hydrogen bonding in the network through introducing an –OH group adjacent to the Schiff-base centers [223]. Jiang et al. [224] synthesized an imine-linked COF that is stable in water and under strong acids and bases by incorporating methoxy groups (-OCH_3) into the pore walls to reinforce interlayer interactions. The introduction of two electron-donating – OCH_3 groups to each phenyl edge delocalized the two lone pairs from the oxygen atom over to the central phenyl ring. In this way, the interlayer interaction was reinforced, and the COF structure was stabilized. This COF demonstrated a high thermal stability up to 673 K, together with a strong resistance towards boiling water, 12 M HCl, 14 M NaOH and common solvents, such as DMF, DMSO, THF, MeOH and cyclohexanone. Recently, Qiu et al. [225] also reported a polyarylether-based COF with a strong resistance towards boiling water, strong acid and bases, oxidation and reduction conditions. Its ultra-high stability was attributed to the inert nature of polyarylether-based building blocks.

For the fabrication of COF-based MMMs, COFs were initially incorporated into polymers to improve the gas permeability of purely polymeric membrane. In such a context, Zhao et al. [226] reported the fabrication of MMMs by incorporating two water-stable COF nanosheets (NUS-2 and NUS-3) into a poly(ether imide) (Ultem) and polybenzimidazole (PBI). As previously indicated, the COF fillers exhibit an excellent compatibility with the polymer matrix, as indicated by the homogeneous texture of the resulting MMMs. Interestingly, the 20 wt % NUS-2@PBI MMM showed a H_2/CO_2 selectivity of 31.4, a value which exceeds the 2008 Robeson upper bound. Later, Shan et al. [16,17] incorporated a stable azine-linked COF (ACOF-1) into Matrimid™ 5218, 6FDA-DAM or Polyactive™ to construct MMMs for CO_2/CH_4 and CO_2/N_2 separation applications. The best performance was observed for the MMMs made of Matrimid, showing more than higher CO_2 permeability and CO_2/N_2 selectivity at 16 wt% of COF loading. Also, Tan et al. [227] prepared 2D-COF based MMMs from π-conjugated viologen-COF precursors and PEO monomers through an in situ bottom-up growth method. The resulting MMMs exhibited exceptional one-month operational stability with a CO_2 permeability of about 772.7 Barrer.

Recently, Zhao et al. [228] combined a 3D COF (COF-300) with two different polymer matrices, including 6FDA-DAM and Pebax-10, to prepare defect-free MMMs due to the good polymer-filler interfacial compatibility. Notably, both membranes exhibited good anti-moisture (relative humidity: 85 %) performance, accompanied by an impressive stability for CO_2/CH_4 separation after continuous operation up to 100 h. Jiang et al. [229] used an imidazolium-based ionic liquid [bmim][Tf_2N]-modified COF-300 as fillers and blended the composite particles IL@COF-300 in Pebax® MH 1657 matrix to synthesize MMMs for CO_2/CH_4 separation. The resultant 7 wt% IL@COF-300/Pebax MMMs showed an excellent CO_2 permeability of 1601 Barrer, together with good stability over 60 days at 1 bar in humidified state. One year later, they also prepared PEG@COF-3/Pebax MMMs that showed a stable CO_2/CH_4 separation performance during a 144 h operation test [57].

In addition to free-standing symmetric COF-based MMMs, thin composite asymmetric COF MMMs have also been reported for CO_2 separation. Jin et al. [230] successfully obtained a honeycomb-like COF-nanosheet cluster with a high CO_2/N_2 adsorption selectivity through a facile mechanical synthesis method. Furthermore, the as-prepared PEBA based MMMs containing only 1 wt% of these COF nanosheet filler could reach a CO_2/N_2 mixed gas selectivity of 72. More importantly, a decent stability was obtained for 120 h of operation (Fig. 10).

6.2. Continuous COF membranes

Besides MMMs, the direct growth of a continuous COF film layer on an appropriate mechanical support through solvothermal approach or interfacial polymerization to prepare thin composites membranes is an alternative to scale up COF membranes [231–235]. However, most of this research has focused on applications in nanofiltration or water treatment. Few studies on COF membranes targeted gas separation because of the remarkably larger pore size of COFs compared to the kinetic diameter of gas molecules. Ben et al. [236] first came up with the idea to grow a COF layer on top of a MOF membrane to prepare COF-MOF composite membranes with the purpose to increase the H_2/CO_2 selectivity compared to their individual counterparts. However, the improvement (from 6 and 7–9 for individual COF and MOF membrane, respectively, to 12–14 for COF-MOF composite MMMs) was not as high as expected.

The same authors further prepared a COF-based composite membrane through strong chemical bonding of a MOF film to a COF layer in the vertical direction. The hybrid membrane achieved a H_2/CO_2 gas mixture selectivity of 32.9 and an ultrahigh H_2 permeability, significantly superior to the state-of-the-art membranes [237]. Inspired by the staggered stacking mode of 2D COFs, Caro et al. [238] developed a novel COF–COF bilayer membrane by growing COF-LZU1 (LZU stands for Lanzhou University) on top of an azine-linked ACOF-1 membrane. Due to the hexagonal pore structure of both COFs, the COF-LZU1-ACOF-1 bilayer membrane is in an appropriate size range of the kinetic diameters of gas molecules by forming interlaced pores. The COF–COF membrane exhibited an excellent separation performance towards H_2/CH_4, H_2/N_2, H_2/CO_2 with selectivity of 100, 84 and 24, respectively, together with a high thermal and long-term operational stability, indicating the great promise of using COF membranes for H_2 production and purification. Similarly, Zhao et al. [239] reported a multilayer COF membranes prepared by a layer-by-layer interfacial crystallization of two COFs (TpPa-SO_3H and $TpTG_{Cl}$) with distinct apertures atop the COF (COF-LZU1) film gutter layer. These composite membranes showed

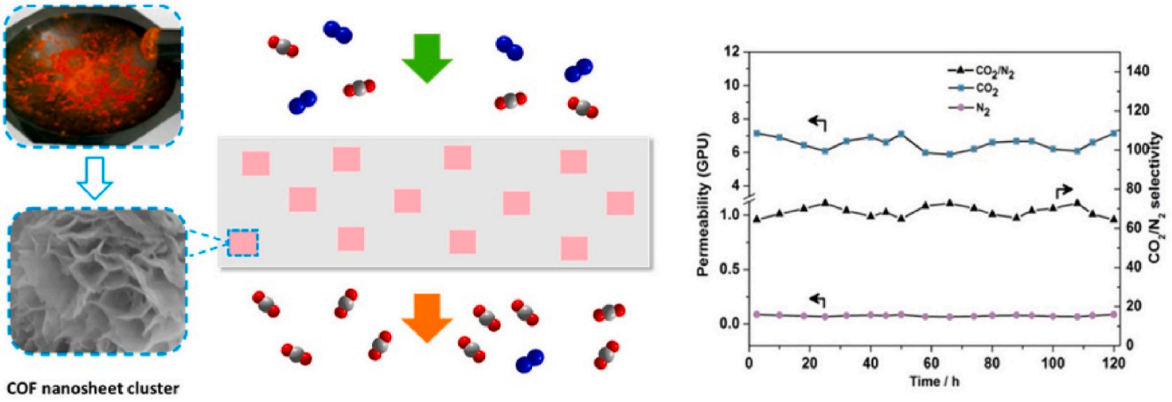

Fig. 10. COF nanosheets cluster based MMMs for CO_2/N_2 separation (equimolar CO_2/N_2 mixture, tested at room temperature and 1 bar). Reproduced with permission from ref. 230, Copyright 2017, Elsevier.

narrowed pores at the COF–COF interfaces, desirable H2/CO2 separation performance and outstanding hydrothermal stability under long continuous testing cycles of dry-humid feed conditions for 96 h.

To better control the stacking modes and maximize the membrane separation performance, Zhao et al. [240] stacked two ionic COF nanosheets (iCONs) with opposite charges to generate strong interlayer interactions through electrostatic attractive interactions between two COF layers. This approach allowed the formation of ultrathin membranes with reduced apertures that showed high H_2 permeance (~2566 GPU) and H_2/CO_2 separation factor (~23), together with an excellent long-term stability under dry or wet conditions at 423 K. Recently, Caro et al. [241] reported another approach that uses the COF interlayer spacing to separate gas mixtures. These authors to successfully grew vertically-aligned COF layers inside vertical CoAl-layered double hydroxide (LDH) nanosheets. The resulting vertical COF membrane exhibited appreciable selectivity towards H_2/CO_2 (31.6) and H_2/CH_4 (29.5), accompanied by an appropriate long-term stability at room temperature (Fig. 11). Although COF membranes used for CO_2 separation have been reported, the long-term stability of COF membrane under realistic conditions are still very limited, more efforts should be devoted to this field.

7. Conclusions

In this review, we have summarized MOFs, MOF-based mixed matrix membranes and methods to improve their stability. In addition, the scalable synthesis of some MOFs and MOF-based membranes was also reviewed. Pioneering work has yet demonstrated stable performance for particular MOF-based MMMs for long duration under dry feed gas steams or water-containing feed. Some pioneering work even reported the CO_2 separation performance of MOF-based MMMs under industrial relevant conditions for which the feed contains water moisture, SO_2, CO, O_2, and NO_X. However, a very limited number of MOF MMMs have been tested under such harsh conditions, and those stability tests only report data up to 100 h. Some MOF-based MMMs could achieve stable performance over 1000 h, though these were only evaluated under dry conditions. Hence, there is still a long way to apply MOF-based MMMs in industry. For example, practical strategies such as coating them with a hydrophobic protective layer need to be implemented to improve their stability. In addition, some studies have demonstrated that the incorporation of MOFs could well improve the stability or plasticization resistance of polymer membranes. Thus, future research should focus more on how to control the interaction between both MOF and polymer chains to improve membranes physical aging and plasticization-resistant properties.

In addition to stability, processability is also an important factor for

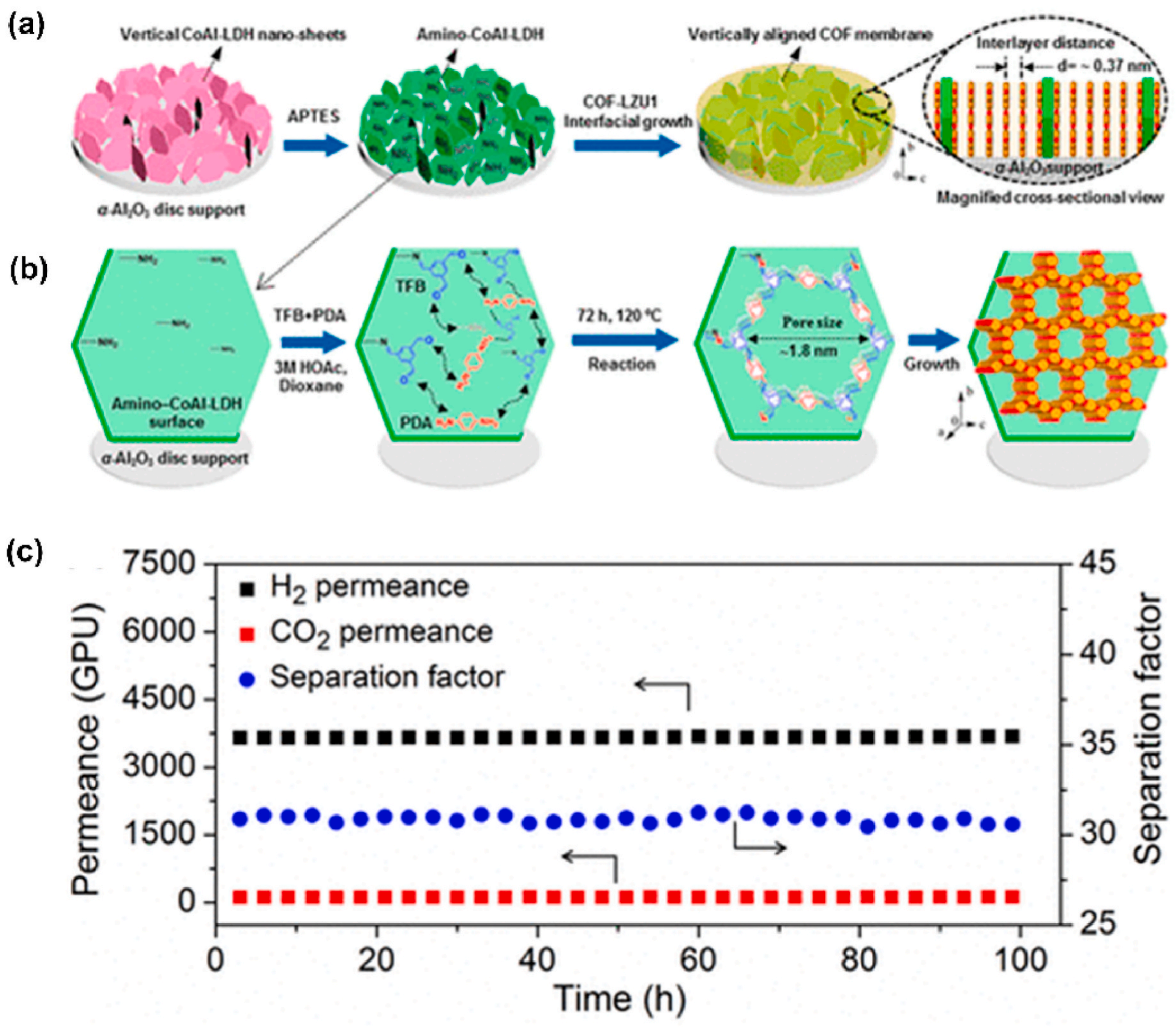

Fig. 11. (a) Schematic representation of the engineering of a vertically aligned COF membrane; (b) Magnified scheme showing the growth of the 2D COF-LZU1 parallel to the surface of a hexagon-shaped amino-CoAl-LDH Nanosheets. (c) Long-term test of the vertically aligned COFLZU1 membrane for equimolar H_2/CO_2 mixture. All measurements at 298 K and 1 bar. Reproduced with permission from ref. 241, Copyright 2020, American Chemical Society.

large-scale manufacturing MOF-based MMMs. Solution processable of MOF fillers is the future direction for preparing MMMs. Finally, as a new emerging filler in MMMs, COFs have already demonstrated better compatibility and stability than MOFs. However, the scale up synthesis of COFs is still at the infancy stage. Effective methods for large scale synthesis of COF fillers are needed; for example, green synthesis conditions, like non-hazardous raw material or solvents, low temperature and pressure should be tried to realize rapid and scalable COF synthesis. With the rapid development of materials synthesis technology, we believe that these problems will be tackled, and MOF- and COF-based MMMs will encounter a blooming development.

Declaration of competing interest

The authors declare the following financial interests/personal relationships which may be considered as potential competing interests: David Vermaas, Inhar Imaz, Thijs Peters, Marcel Boerrigter reports financial support was provided by European Union. Meixia Shan reports financial support was provided by National Natural Science Foundation of China. Meixia Shan, Xiumei Geng reports financial support was provided by China Postdoctoral Science Foundation. Inhar Imaz, Daniel Maspoch, Anna Broto-Ribas, Borja Ortin-Rubio reports financial support was provided by Government of Catalonia.

Data availability

No data was used for the research described in the article.

Acknowledgments

The authors acknowledge financial support from the European Union's Horizon 2020 research and innovation program under grant agreement No 760899, the National Natural Science Foundation of China (Nos. 52003250) and China Postdoctoral Science Foundation (No. 2020M682351). This work was also supported by the Catalan AGAUR (project 2017 SGR 238) and the CERCA Program/Generalitat de Catalunya. ICN2 is supported by the Severo Ochoa program from the Spanish MINECO (grant SEV-2017-0706).

References

[1] R.S. Haszeldine, Carbon capture and storage: how green can black Be? Science 325 (5948) (2009) 1647–1652.
[2] B.P. Spigarelli, S.K. Kawatra, Opportunities and challenges in carbon dioxide capture, J. CO_2 Util. 1 (2013) 69–87.
[3] B. Seoane, J. Coronas, I. Gascon, M.E. Benavides, O. Karvan, J. Caro, F. Kapteijn, J. Gascon, Metal-organic framework based mixed matrix membranes: a solution for highly efficient CO_2 capture? Chem. Soc. Rev. 44 (8) (2015) 2421–2454.
[4] R. M, William J. Koros, Pushing the limits on possibilities for large scale gas separation: which strategies? J. Membr. Sci. 175 (2) (2000) 181–196.
[5] X. He, M.B. Hagg, Membranes for environmentally friendly energy processes, Membranes 2 (4) (2012) 706–726.
[6] L.M. Robeson, The upper bound revisited, J. Membr. Sci. 320 (1–2) (2008) 390–400.
[7] H.B. Park, J. Kamcev, L.M. Robeson, M. Elimelech, B.D. Freeman, Maximizing the right stuff: the trade-off between membrane permeability and selectivity, Science 356 (6343) (2017) 1138–1148.
[8] J.E. Bachman, J.R. Long, Plasticization-resistant Ni_2(dobdc)/polyimide composite membranes for the removal of CO_2 from natural gas, Energy Environ. Sci. 9 (6) (2016) 2031–2036.
[9] J.E. Bachman, Z.P. Smith, T. Li, T. Xu, J.R. Long, Enhanced ethylene separation and plasticization resistance in polymer membranes incorporating metal-organic framework nanocrystals, Nat. Mater. 15 (8) (2016) 845–849.
[10] H. Lin, E.V. Wagner, B.D. Freeman, L.G. Toy, R.P. Gupta, Plasticization-enhanced hydrogen purification using polymeric membranes, Science 311 (5761) (2006) 639–642.
[11] Z.X. Low, P.M. Budd, N.B. McKeown, D.A. Patterson, Gas permeation properties, physical aging, and its mitigation in high free volume glassy polymers, Chem. Rev. 118 (12) (2018) 5871–5911.
[12] D.Q. Vu, W.J. Koros, S.J. Miller, Mixed matrix membranes using carbon molecular sieves: I. Preparation and experimental results, J. Membr. Sci. 211 (2) (2003) 311–334.
[13] M.M. Khan, V. Filiz, G. Bengtson, S. Shishatskiy, M.M. Rahman, J. Lillepaerg, V. Abetz, Enhanced gas permeability by fabricating mixed matrix membranes of functionalized multiwalled carbon nanotubes and polymers of intrinsic microporosity (PIM), J. Membr. Sci. 436 (2013) 109–120.
[14] B. Zornoza, O. Esekhile, W.J. Koros, C. Téllez, J. Coronas, Hollow silicalite-1 sphere-polymer mixed matrix membranes for gas separation, Sep. Purif. Technol. 77 (1) (2011) 137–145.
[15] A.M.W. Hillock, S.J. Miller, W.J. Koros, Crosslinked mixed matrix membranes for the purification of natural gas: effects of sieve surface modification, J. Membr. Sci. 314 (1–2) (2008) 193–199.
[16] M. Shan, B. Seoane, E. Rozhko, A. Dikhtiarenko, G. Clet, F. Kapteijn, J. Gascon, Azine-linked covalent organic framework (COF)-Based mixed-matrix membranes for CO_2/CH_4 separation, Chem. Eur J. 22 (41) (2016) 14467–14470.
[17] M. Shan, B. Seoane, E. Andres-Garcia, F. Kapteijn, J. Gascon, Mixed-matrix membranes containing an azine-linked covalent organic framework: influence of the polymeric matrix on post-combustion CO_2-capture, J. Membr. Sci. 549 (2018) 377–384.
[18] B.P. Biswal, H.D. Chaudhari, R. Banerjee, U.K. Kharul, Chemically stable covalent organic framework (COF)-Polybenzimidazole hybrid membranes: enhanced gas separation through pore modulation, Chem. Eur J. 22 (14) (2016) 4695–4699.
[19] T. Rodenas, I. Luz, G. Prieto, B. Seoane, H. Miro, A. Corma, F. Kapteijn, F. X. Llabrés i Xamena, J. Gascon, Metal–organic framework nanosheets in polymer composite materials for gas separation, Nat. Mater. 14 (1) (2015) 48–55.
[20] B. Zornoza, A. Martinez-Joaristi, P. Serra-Crespo, C. Tellez, J. Coronas, J. Gascon, F. Kapteijn, Functionalized flexible MOFs as fillers in mixed matrix membranes for highly selective separation of CO_2 from CH_4 at elevated pressures, Chem. Commun. 47 (33) (2011) 9522–9524.
[21] X. Liu, Y. Li, G. Zhu, Y. Ban, L. Xu, W. Yang, An organophilic pervaporation membrane derived from metal-organic framework nanoparticles for efficient recovery of bio-alcohols, Angew. Chem. Int. Ed. 50 (45) (2011) 10636–10639.
[22] A. Pustovarenko, M.G. Goesten, S. Sachdeva, M. Shan, Z. Amghouz, Y. Belmabkhout, A. Dikhtiarenko, T. Rodenas, D. Keskin, I.K. Voets, B. M. Weckhuysen, M. Eddaoudi, L. de Smet, E.J.R. Sudholter, F. Kapteijn, B. Seoane, J. Gascon, Nanosheets of nonlayered aluminum metal-organic frameworks through a surfactant-assisted method, Adv. Mater. 30 (26) (2018), 1707234.
[23] N. Tien-Binh, D. Rodrigue, S. Kaliaguine, In-situ cross interface linking of PIM-1 polymer and UiO-66-NH_2 for outstanding gas separation and physical aging control, J. Membr. Sci. 548 (2018) 429–438.
[24] Z. Wang, D. Wang, S. Zhang, L. Hu, J. Jin, Interfacial design of mixed matrix membranes for improved gas separation performance, Adv. Mater. 28 (17) (2016) 3399–3405.
[25] B. Zornoza, C. Téllez, J. Coronas, O. Esekhile, W.J. Koros, Mixed matrix membranes based on 6FDA polyimide with silica and zeolite microsphere dispersed phases, AIChE J. 61 (12) (2015) 4481–4490.
[26] B. Ghalei, K. Sakurai, Y. Kinoshita, K. Wakimoto, A.P. Isfahani, Q. Song, K. Doitomi, S. Furukawa, H. Hirao, H. Kusuda, S. Kitagawa, E. Sivaniah, Enhanced selectivity in mixed matrix membranes for CO_2 capture through efficient dispersion of amine-functionalized MOF nanoparticles, Nat. Energy 2 (7) (2017), 17086.
[27] Z. Wang, H. Ren, S. Zhang, F. Zhang, J. Jin, Polymers of intrinsic microporosity/metal–organic framework hybrid membranes with improved interfacial interaction for high-performance CO_2 separation, J. Mater. Chem. A 5 (22) (2017) 10968–10977.
[28] G. Chen, C. Chen, Y. Guo, Z. Chu, Y. Pan, G. Liu, G. Liu, Y. Han, W. Jin, N. Xu, Solid-solvent processing of ultrathin, highly loaded mixed-matrix membrane for gas separation, Science 381 (6664) (2023) 1350–1356.
[29] X. Zhao, Y. Wang, D.-S. Li, X. Bu, P. Feng, Metal–organic frameworks for separation, Adv. Mater. 30 (37) (2018), 1705189.
[30] X. Wang, C. Chi, K. Zhang, Y. Qian, K.M. Gupta, Z. Kang, J. Jiang, D. Zhao, Reversed thermo-switchable molecular sieving membranes composed of two-dimensional metal-organic nanosheets for gas separation, Nat. Commun. 8 (2017), 14460.
[31] H. Li, Y. Yin, L. Zhu, Y. Xiong, X. Li, T. Guo, W. Xing, Q. Xue, A hierarchical structured steel mesh decorated with metal organic framework/graphene oxide for high-efficient oil/water separation, J. Hazard Mater. 373 (2019) 725–732.
[32] A. Sabetghadam, X. Liu, M. Benzaqui, E. Gkaniatsou, A. Orsi, M.M. Lozinska, C. Sicard, T. Johnson, N. Steunou, P.A. Wright, C. Serre, J. Gascon, F. Kapteijn, Influence of filler pore structure and polymer on the performance of MOF-based mixed-matrix membranes for CO_2 capture, Chem. Eur J. 24 (31) (2018) 7949–7956.
[33] A. Sabetghadam, X. Liu, S. Gottmer, L. Chu, J. Gascon, F. Kapteijn, Thin mixed matrix and dual layer membranes containing metal-organic framework nanosheets and Polyactive™ for CO_2 capture, J. Membr. Sci. 570–571 (2019) 226–235.
[34] M. Ahmadi, S. Janakiram, Z. Dai, L. Ansaloni, L. Deng, Performance of mixed matrix membranes containing porous two-dimensional (2D) and three-dimensional (3D) fillers for CO_2 separation: a review, Membranes 8 (3) (2018) 50.
[35] A. Knebel, J. Caro, Metal-organic frameworks and covalent organic frameworks as disruptive membrane materials for energy-efficient gas separation, Nat. Nanotechnol. 17 (9) (2022) 911–923.
[36] A. Kertik, L.H. Wee, M. Pfannmöller, S. Bals, J.A. Martens, I.F.J. Vankelecom, Highly selective gas separation membrane using in situ amorphised metal–organic frameworks, Energy Environ. Sci. 10 (11) (2017) 2342–2351.
[37] M.S. Denny Jr., J.C. Moreton, L. Benz, S.M. Cohen, Metal–organic frameworks for membrane-based separations, Nat. Rev. Mater. 1 (2016), 16078.

[38] A.J. Howarth, Y. Liu, P. Li, Z. Li, T.C. Wang, J.T. Hupp, O.K. Farha, Chemical, thermal and mechanical stabilities of metal–organic frameworks, Nat. Rev. Mater. 1 (2016), 15018.

[39] H. Furukawa, K.E. Cordova, M. O'Keeffe, O.M. Yaghi, The chemistry and applications of metal-organic frameworks, Science 341 (6149) (2013), 1230444.

[40] H. Li, M. Eddaoudi, M. O'Keeffe, O.M. Yaghi, Design and synthesis of an exceptionally stable and highly porous metal-organic framework, Nature 402 (1999) 276–279.

[41] S. Kanehashi, A. Aguiar, H.T. Lu, G.Q. Chen, S.E. Kentish, Effects of industrial gas impurities on the performance of mixed matrix membranes, J. Membr. Sci. 549 (2018) 686–692.

[42] Z. Li, F. Liao, F. Jiang, B. Liu, S. Ban, G. Chen, C. Sun, P. Xiao, Y. Sun, Capture of H_2S and SO_2 from trace sulfur containing gas mixture by functionalized UiO-66 (Zr) materials: a molecular simulation study, Fluid Phase Equil. 427 (2016) 259–267.

[43] O. Shekhah, Y. Belmabkhout, Z. Chen, V. Guillerm, A. Cairns, K. Adil, M. Eddaoudi, Made-to-order metal-organic frameworks for trace carbon dioxide removal and air capture, Nat. Commun. 5 (2014) 4228.

[44] M. Kandiah, M.H. Nilsen, S. Usseglio, S. Jakobsen, U. Olsbye, M. Tilset, C. Larabi, E.A. Quadrelli, F. Bonino, K.P. Lillerud, Synthesis and stability of tagged UiO-66 Zr-MOFs, Chem. Mater. 22 (24) (2010) 6632–6640.

[45] S. Yuan, J.S. Qin, C.T. Lollar, H.C. Zhou, Stable metal-organic frameworks with group 4 metals: current status and trends, ACS Cent. Sci. 4 (4) (2018) 440–450.

[46] Z. Zhang, Z.-Z. Yao, S. Xiang, B. Chen, Perspective of microporous metal–organic frameworks for CO_2 capture and separation, Energy Environ. Sci. 7 (9) (2014) 2868–2899.

[47] Z. Kang, L. Fan, D. Sun, Recent advances and challenges of metal–organic framework membranes for gas separation, J. Mater. Chem. A 5 (21) (2017) 10073–10091.

[48] R. Lin, B.V. Hernandez, L. Ge, Z. Zhu, Metal organic framework based mixed matrix membranes: an overview on filler/polymer interfaces, J. Mater. Chem. A 6 (2) (2018) 293–312.

[49] Q. Qian, P.A. Asinger, M.J. Lee, G. Han, K. Mizrahi Rodriguez, S. Lin, F. M. Benedetti, A.X. Wu, W.S. Chi, Z.P. Smith, MOF-based membranes for gas separations, Chem. Rev. 120 (16) (2020) 8161–8266.

[50] Z. Kang, H. Guo, L. Fan, G. Yang, Y. Feng, D. Sun, S. Mintova, Scalable crystalline porous membranes: current state and perspectives, Chem. Soc. Rev. 50 (3) (2021) 1913–1944.

[51] M.Z. Ahmad, T.A. Peters, N.M. Konnertz, T. Visser, C. Téllez, J. Coronas, V. Fila, W.M. de Vos, N.E. Benes, High-pressure CO_2/CH_4 separation of Zr-MOFs based mixed matrix membranes, Sep. Purif. Technol. 230 (2020), 115858.

[52] Z. Lai, Development of ZIF-8 membranes: opportunities and challenges for commercial applications, Curr. Opin. Chem. Eng. 20 (2018) 78–85.

[53] X. Liu, X. Wang, F. Kapteijn, Water and metal–organic frameworks: from interaction toward utilization, Chem. Rev. 120 (16) (2020) 8303–8377.

[54] R. Freund, O. Zaremba, G. Arnauts, R. Ameloot, G. Skorupskii, M. Dincă, A. Bavykina, J. Gascon, A. Ejsmont, J. Gościańska, M. Kalmutzki, U. Lächelt, E. Ploetz, C. Diercks, S. Wuttke, The current status of MOF and COF applications, Angew. Chem. Int. Ed. 60 (45) (2021) 23975–24001.

[55] Y. Cheng, S.J. Datta, S. Zhou, J. Jia, O. Shekhah, M. Eddaoudi, Advances in metal-organic framework-based membranes, Chem. Soc. Rev. 51 (19) (2022) 8300–8350.

[56] L. Hu, K. Clark, T. Alebrahim, H. Lin, Mixed matrix membranes for post-combustion carbon capture: from materials design to membrane engineering, J. Membr. Sci. 644 (2022).

[57] Y. Liu, H. Wu, S. Wu, S. Song, Z. Guo, Y. Ren, R. Zhao, L. Yang, Y. Wu, Z. Jiang, Multifunctional covalent organic framework (COF)-Based mixed matrix membranes for enhanced CO_2 separation, J. Membr. Sci. 618 (2021), 118693.

[58] J. Lee, S. Hong, H. Cho, B. Lyu, M. Kim, J. Kim, I. Moon, Machine learning-based energy optimization for on-site SMR hydrogen production, Energy Convers. Manag. 244 (2021), 114438.

[59] H.T. Lu, S. Kanehashi, C.A. Scholes, S.E. Kentish, The potential for use of cellulose triacetate membranes in post combustion capture, Int. J. Greenh. Gas Control 55 (2016) 97–104.

[60] R. Anantharaman, O. Bolland, N. Booth, E.v. Dorst, C. Ekstrom, E.S. Fernandes, F. Franco, E. Macchi, G. Manzolini, D. Nikolic, A. Pfeffer, M. Prins, S. Rezvani, L. Robinson, European Best Practice Guidelines for Assessment of CO_2 Capture Technologies, DECARBit Consortium, 2011.

[61] C. Zhang, R.S. Patil, T. Li, C.L. Barnes, S.J. Teat, J.L. Atwood, Preparation of magnesium-seamed C-Alkylpyrogallol[4]arene nanocapsules with varying chain lengths, Chemistry 23 (35) (2017) 8520–8524.

[62] X.Y. Chen, H. Vinh-Thang, A.A. Ramirez, D. Rodrigue, S. Kaliaguine, Membrane gas separation technologies for biogas upgrading, RSC Adv. 5 (31) (2015) 24399–24448.

[63] T. Islamoglu, Z. Chen, M.C. Wasson, C.T. Buru, K.O. Kirlikovali, U. Afrin, M. R. Mian, O.K. Farha, Metal-organic frameworks against toxic chemicals, Chem. Rev. 120 (16) (2020) 8130–8160.

[64] S.S. Kaye, A. Dailly, O.M. Yaghi, J.R. Long, Impact of preparation and handling on the hydrogen storage properties of Zn_4O(1,4-benzenedicarboxylate)$_3$ (MOF-5), J. Am. Chem. Soc. 129 (46) (2007) 14176–14177.

[65] J.G. Nguyen, S.M. Cohen, Moisture-resistant and superhydrophobic metal-organic frameworks obtained via postsynthetic modification, J. Am. Chem. Soc. 132 (13) (2010) 4560–4561.

[66] K. Xie, Q. Fu, J. Kima, H. Lu, Y. He, Q. Zhao, J. Scofield, P.A. Webley, G.G. Qiao, Increasing both selectivity and permeability of mixed-matrix membranes: sealing the external surface of porous MOF nanoparticles, J. Membr. Sci. 535 (2017) 350–356.

[67] G.W. Peterson, G.W. Wagner, A. Balboa, J. Mahle, T. Sewell, C.J. Karwacki, Ammonia vapor removal by $Cu_3(BTC)_2$ and its characterization by MAS NMR, J. Phys. Chem. C 113 (31) (2009) 13906–13917.

[68] D. Saha, S. Deng, Ammonia adsorption and its effects on framework stability of MOF-5 and MOF-177, J. Colloid Interface Sci. 348 (2) (2010) 615–620.

[69] J. Ethiraj, F. Bonino, C. Lamberti, S. Bordiga, H_2S interaction with HKUST-1 and ZIF-8 MOFs: a multitechnique study, Microporous Mesoporous Mater. 207 (2015) 90–94.

[70] K.S. Park, Z. Ni, A.P. Côté, J.Y. Choi, R. Huang, F.J. Uribe-Romo, H.K. Chae, M. O'Keeffe, O.M. Yaghi, Exceptional chemical and thermal stability of zeolitic imidazolate frameworks, Proc. Natl. Acad. Sci. USA 103 (27) (2006) 10186–10191.

[71] X. Liu, Y. Li, Y. Ban, Y. Peng, H. Jin, H. Bux, L. Xu, J. Caro, W. Yang, Improvement of hydrothermal stability of zeolitic imidazolate frameworks, Chem. Commun. (Camb.) 49 (80) (2013) 9140–9142.

[72] J. Liu, A.I. Benin, A.M. Furtado, P. Jakubczak, R.R. Willis, M.D. LeVan, Stability effects on CO_2 adsorption for the DOBDC series of metal-organic frameworks, Langmuir 27 (18) (2011) 11451–11456.

[73] K. Tan, S. Zuluaga, Q. Gong, Y. Gao, N. Nijem, J. Li, T. Thonhauser, Y.J. Chabal, Competitive co-adsorption of CO_2 with H_2O, NH_3, SO_2, NO, NO_2, N_2, O_2, and CH_4 in M-MOF-74 (M= Mg, Co, Ni): the role of hydrogen bonding, Chem. Mater. 27 (6) (2015) 2203–2217.

[74] J.H. Cavka, S. Jakobsen, U. Olsbye, N. Guillou, C. Lamberti, S. Bordiga, K. P. Lillerud, A new zirconium inorganic building brick forming metal organic frameworks with exceptional stability, J. Am. Chem. Soc. 130 (42) (2008) 13850–13851.

[75] F. Jeremias, A. Khutia, S.K. Henninger, C. Janiak, MIL-100(Al, Fe) as water adsorbents for heat transformation purposes—a promising application, J. Mater. Chem. A 22 (20) (2012) 10148–10151.

[76] H. Kummer, F. Jeremias, A. Warlo, G. Füdner, D. Fröhlich, C. Janiak, R. Gläser, S. K. Henninger, A functional full-scale heat exchanger coated with aluminum fumarate Metal−Organic framework for adsorption heat transformation, Ind. Eng. Chem. Res. 56 (29) (2017) 8393–8398.

[77] F. Ragon, B. Campo, Q. Yang, C. Martineau, A.D. Wiersum, A. Lago, V. Guillerm, C. Hemsley, J.F. Eubank, M. Vishnuvarthan, F. Taulelle, P. Horcajada, A. Vimont, P.L. Llewellyn, M. Daturi, S. Devautour-Vinot, G. Maurin, C. Serre, T. Devic, G. Clet, Acid-functionalized UiO-66(Zr) MOFs and their evolution after intra-framework cross-linking: structural features and sorption properties, J. Mater. Chem. A 3 (7) (2015) 3294–3309.

[78] J.N. Joshi, G. Zhu, J.J. Lee, E.A. Carter, C.W. Jones, R.P. Lively, K.S. Walton, Probing metal–organic framework design for adsorptive natural gas purification, Langmuir 34 (29) (2018) 8443–8450.

[79] D. Fröhlich, E. Pantatosaki, P.D. Kolokathis, K. Markey, H. Reinsch, M. Baumgartner, M.A. van der Veen, D.E. De Vos, N. Stock, G.K. Papadopoulos, S. K. Henninger, C. Janiak, Water adsorption behaviour of CAU-10-H: a thorough investigation of its structure–property relationships, J. Mater. Chem. A 4 (30) (2016) 11859–11869.

[80] Y. Khabzina, J. Dhainaut, M. Ahlhelm, H.-J. Richter, H. Reinsch, N. Stock, D. Farrusseng, Synthesis and shaping scale-up study of functionalized UiO-66 MOF for ammonia air purification filters, Ind. Eng. Chem. Res. 57 (24) (2018) 8200–8208.

[81] J.H. Carter, X. Han, F.Y. Moreau, I. da Silva, A. Nevin, H.G.W. Godfrey, C.C. Tang, S. Yang, M. Schroder, Exceptional adsorption and binding of sulfur dioxide in a robust zirconium-based metal-organic framework, J. Am. Chem. Soc. 140 (46) (2018) 15564–15567.

[82] S. Nandi, H. Reinsch, S. Biswas, A vinyl functionalized mixed linker CAU-10 metal-organic framework acting as a fluorescent sensor for the selective detection of H_2S and palladium(II), Microporous Mesoporous Mater. 293 (2020), 109790.

[83] N. Tannert, C. Jansen, S. Nießing, C. Janiak, Robust synthesis routes and porosity of the Al-based metal–organic frameworks Al-fumarate, CAU-10-H and MIL-160, Dalton Trans. 48 (9) (2019) 2967–2976.

[84] A.J. Rieth, M. Dincă, Controlled gas uptake in metal–organic frameworks with record ammonia sorption, J. Am. Chem. Soc. 140 (9) (2018) 3461–3466.

[85] A.J. Rieth, S. Yang, E.N. Wang, M. Dincă, Record atmospheric fresh water capture and heat transfer with a material operating at the water uptake reversibility limit, ACS Cent. Sci. 3 (6) (2017) 668–672.

[86] L.M. Rodriguez-Albelo, E. Lopez-Maya, S. Hamad, A.R. Ruiz-Salvador, S. Calero, J.A. Navarro, Selective sulfur dioxide adsorption on crystal defect sites on an isoreticular metal organic framework series, Nat. Commun. 8 (2017), 14457.

[87] N.C. Burtch, H. Jasuja, K.S. Walton, Water stability and adsorption in metal-organic frameworks, Chem. Rev. 114 (20) (2014) 10575–10612.

[88] H.J. Choi, M. Dincă, A. Dailly, J.R. Long, Hydrogen storage in water-stable metal–organic frameworks incorporating 1,3- and 1,4-benzenedipyrazolate, Energy Environ. Sci. 3 (1) (2010) 117–123.

[89] V. Colombo, S. Galli, H.J. Choi, G.D. Han, A. Maspero, G. Palmisano, N. Masciocchi, J.R. Long, High thermal and chemical stability in pyrazolate-bridged metal–organic frameworks with exposed metal sites, Chem. Sci. 2 (7) (2011) 1311–1319.

[90] D. Feng, Z.-Y. Gu, J.-R. Li, H.-L. Jiang, Z. Wei, H.-C. Zhou, Zirconium-metalloporphyrin PCN-222: mesoporous metal–organic frameworks with ultrahigh stability as biomimetic catalysts, Angew. Chem. Int. Ed. 51 (41) (2012) 10307–10310.

[91] T.-F. Liu, D. Feng, Y.-P. Chen, L. Zou, M. Bosch, S. Yuan, Z. Wei, S. Fordham, K. Wang, H.-C. Zhou, Topology-guided design and syntheses of highly stable

mesoporous porphyrinic zirconium metal–organic frameworks with high surface area, J. Am. Chem. Soc. 137 (1) (2015) 413–419.

[92] J.M. Taylor, R. Vaidhyanathan, S.S. Iremonger, G.K.H. Shimizu, Enhancing water stability of metal–organic frameworks via phosphonate monoester linkers, J. Am. Chem. Soc. 134 (35) (2012) 14338–14340.

[93] C. Serre, Superhydrophobicity in highly fluorinated porous metal-organic frameworks, Angew. Chem. Int. Ed. 51 (25) (2012) 6048–6050.

[94] T.H. Chen, I. Popov, O. Zenasni, O. Daugulis, O.S. Miljanic, Superhydrophobic perfluorinated metal-organic frameworks, Chem. Commun. 49 (61) (2013) 6846–6848.

[95] T. Li, D.-L. Chen, J.E. Sullivan, M.T. Kozlowski, J.K. Johnson, N.L. Rosi, Systematic modulation and enhancement of $CO_2 : N_2$ selectivity and water stability in an isoreticular series of bio-MOF-11 analogues, Chem. Sci. 4 (4) (2013) 1746–1755.

[96] S.J. Yang, C.R. Park, Preparation of highly moisture-resistant black-colored metal organic frameworks, Adv. Mater. 24 (29) (2012) 4010–4013.

[97] W. Zhang, Y. Hu, J. Ge, H.L. Jiang, S.H. Yu, A facile and general coating approach to moisture/water-resistant metal–organic frameworks with intact porosity, J. Am. Chem. Soc. 136 (49) (2014) 16978–16981.

[98] J. Gascon, S. Aguado, F. Kapteijn, Manufacture of dense coatings of $Cu_3(BTC)_2$ (HKUST-1) on α-alumina, Microporous Mesoporous Mater. 113 (1–3) (2008) 132–138.

[99] H. Guo, G. Zhu, I.J. Hewitt, S. Qiu, "Twin copper source" growth of metal-organic framework membrane: $Cu_3(BTC)_2$ with high permeability and selectivity for recycling H_2, J. Am. Chem. Soc. 131 (5) (2009) 1646–1647.

[100] S. Zhou, O. Shekhah, A. Ramirez, P. Lyu, E. Abou-Hamad, J. Jia, J. Li, P.M. Bhatt, Z. Huang, H. Jiang, T. Jin, G. Maurin, J. Gascon, M. Eddaoudi, Asymmetric pore windows in MOF membranes for natural gas valorization, Nature 606 (7915) (2022) 706–712.

[101] H.T. Kwon, H.K. Jeong, A.S. Lee, H.S. An, J.S. Lee, Heteroepitaxially grown zeolitic imidazolate framework membranes with unprecedented propylene/propane separation performances, J. Am. Chem. Soc. 137 (38) (2015) 12304–12311.

[102] Y. Liu, Y. Ban, W. Yang, Microstructural engineering and architectural design of metal–organic framework membranes, Adv. Mater. 29 (31) (2017), 1606949.

[103] X. Liu, C. Wang, B. Wang, K. Li, Novel organic-dehydration membranes prepared from zirconium metal-organic frameworks, Adv. Funct. Mater. 27 (3) (2017), 1604311.

[104] H. Bux, A. Feldhoff, J. Cravillon, M. Wiebcke, Y.-S. Li, J. Caro, Oriented zeolitic imidazolate framework-8 membrane with sharp H_2/C_3H_8 molecular sieve separation, Chem. Mater. 23 (8) (2011) 2262–2269.

[105] B.A. Al-Maythalony, O. Shekhah, R. Swaidan, Y. Belmabkhout, I. Pinnau, M. Eddaoudi, Quest for anionic MOF membranes: continuous sod-ZMOF membrane with CO_2 adsorption-driven selectivity, J. Am. Chem. Soc. 137 (5) (2015) 1754–1757.

[106] A. Huang, W. Dou, J. Caro, Steam-stable zeolitic imidazolate framework ZIF-90 membrane with hydrogen, J. Am. Chem. Soc. 132 (44) (2010) 15562–15564.

[107] Y. Hu, X. Dong, J. Nan, W. Jin, X. Ren, N. Xu, Y.M. Lee, Metal-organic framework membranes fabricated via reactive seeding, Chem. Commun. 47 (2) (2011) 737–739.

[108] A.J. Brown, N.A. Brunelli, K. Eum, F. Rashidi, J.R. Johnson, W.J. Koros, C. W. Jones, S. Nair, Interfacial microfluidic processing of metal-organic framework hollow fiber membranes, Science 345 (6192) (2014) 72–75.

[109] T.J.P.H. Yehia, J.P. Ferraris, K.J. Balkus, I.H. Musselman, Methane facilitated transport using copper(II) biphenyl dicarboxylate-triethylenediamine/poly(3-acetoxyethylthiophene) mixed matrix membranes, Polym. Prepr. (Am. Chem. Soc., Div. Polym. Chem.) 45 (2004) 35–36.

[110] G. Liu, V. Chernikova, Y. Liu, K. Zhang, Y. Belmabkhout, O. Shekhah, C. Zhang, S. Yi, M. Eddaoudi, W.J. Koros, Mixed matrix formulations with MOF molecular sieving for key energy-intensive separations, Nat. Mater. 17 (3) (2018) 283–289.

[111] M.W. Anjum, F. Vermoortele, A.L. Khan, B. Bueken, D.E. De Vos, I.F. Vankelecom, Modulated UiO-66-based mixed-matrix membranes for CO_2 separation, ACS Appl. Mater. Interfaces 7 (45) (2015) 25193–25201.

[112] S. Sorribas, P. Gorgojo, C. Tellez, J. Coronas, A.G. Livingston, High flux thin film nanocomposite membranes based on metal-organic frameworks for organic solvent nanofiltration, J. Am. Chem. Soc. 135 (40) (2013) 15201–15208.

[113] M. Etxeberria-Benavides, T. Johnson, S. Cao, B. Zornoza, J. Coronas, J. Sanchez-Lainez, A. Sabetghadam, X. Liu, E. Andres-Garcia, F. Kapteijn, J. Gascon, O. David, PBI mixed matrix hollow fiber membrane: influence of ZIF-8 filler over H_2/CO_2 separation performance at high temperature and pressure, Sep. Purif. Technol. 237 (2020).

[114] Y. Cheng, X. Wang, C. Jia, Y. Wang, L. Zhai, Q. Wang, D. Zhao, Ultrathin mixed matrix membranes containing two-dimensional metal-organic framework nanosheets for efficient CO_2/CH_4 separation, J. Membr. Sci. 539 (2017) 213–223.

[115] B. Wang, J. Xu, J. Wang, S. Zhao, X. Liu, Z. Wang, High-performance membrane with angstrom-scale manipulation of gas transport channels via polymeric decorated MOF cavities, J. Membr. Sci. 625 (2021).

[116] Y. Cheng, Y. Ying, S. Japip, S.-D. Jiang, T.-S. Chung, S. Zhang, D. Zhao, Advanced porous materials in mixed matrix membranes, Adv. Mater. 30 (47) (2018), 1802401.

[117] V. Nafisi, M.-B. Hägg, Development of dual layer of ZIF-8/PEBAX-2533 mixed matrix membrane for CO_2 capture, J. Membr. Sci. 459 (2014) 244–255.

[118] T. Yang, T.-S. Chung, High performance ZIF-8/PBI nano-composite membranes for high temperature hydrogen separation consisting of carbon monoxide and water vapor, Int. J. Hydrogen Energy 38 (1) (2013) 229–239.

[119] P.D. Sutrisna, J. Hou, H. Li, Y. Zhang, V. Chen, Improved operational stability of Pebax-based gas separation membranes with ZIF-8: a comparative study of flat sheet and composite hollow fibre membranes, J. Membr. Sci. 524 (2017) 266–279.

[120] M. Barooah, B. Mandal, Synthesis, characterization and CO_2 separation performance of novel PVA/PG/ZIF-8 mixed matrix membrane, J. Membr. Sci. 572 (2019) 198–209.

[121] J. Sánchez-Laínez, L. Paseta, M. Navarro, B. Zornoza, C. Téllez, J. Coronas, Ultrapermeable thin film ZIF-8/polyamide membrane for H_2/CO_2 separation at high temperature without using sweep gas, Adv. Mater. Interfac. 5 (19) (2018), 1800647.

[122] A. Guo, Y. Ban, K. Yang, W. Yang, Metal-organic framework-based mixed matrix membranes: synergetic effect of adsorption and diffusion for CO_2/CH_4 separation, J. Membr. Sci. 562 (2018) 76–84.

[123] S. Kanehashi, G.Q. Chen, L. Ciddor, A. Chaffee, S.E. Kentish, The impact of water vapor on CO_2 separation performance of mixed matrix membranes, J. Membr. Sci. 492 (2015) 471–477.

[124] C. Jiao, Z. Li, X. Li, M. Wu, H. Jiang, Improved CO_2/N_2 separation performance of Pebax composite membrane containing polyethyleneimine functionalized ZIF-8, Sep. Purif. Technol. 259 (2021), 118190.

[125] Y. Wang, J. Wang, X. Zhang, J. Li, L. Li, Polyvinylamine/ZIF-8-decorated metakaolin composite membranes for CO_2/N_2 separation, Sep. Purif. Technol. 270 (2021), 118800.

[126] X. Li, S. Yu, K. Li, C. Ma, J. Zhang, H. Li, X. Chang, L. Zhu, Q. Xue, Enhanced gas separation performance of Pebax mixed matrix membranes by incorporating ZIF-8 in situ inserted by multiwalled carbon nanotubes, Sep. Purif. Technol. 248 (2020), 117080.

[127] J. Shen, G. Liu, K. Huang, Q. Li, K. Guan, Y. Li, W. Jin, UiO-66-polyether block amide mixed matrix membranes for CO_2 separation, J. Membr. Sci. 513 (2016) 155–165.

[128] M. Mozafari, R. Abedini, A. Rahimpour, Zr-MOFs-incorporated thin film nanocomposite Pebax 1657 membranes dip-coated on polymethylpentyne layer for efficient separation of CO_2/CH_4, J. Mater. Chem. A 6 (26) (2018) 12380–12392.

[129] R. Xu, Z. Wang, M. Wang, Z. Qiao, J. Wang, High nanoparticles loadings mixed matrix membranes via chemical bridging-crosslinking for CO_2 separation, J. Membr. Sci. 573 (2019) 455–464.

[130] S. Ashtiani, M. Khoshnamvand, D. Bouša, J. Šturala, Z. Sofer, A. Shaliutina-Kolešová, D. Gardenö, K. Friess, Surface and interface engineering in CO_2-philic based UiO-66-NH_2-PEI mixed matrix membranes via covalently bridging PVP for effective hydrogen purification, Int. J. Hydrogen Energy 46 (7) (2021) 5449–5458.

[131] F. Guo, B. Li, R. Ding, D. Li, X. Jiang, G. He, W. Xiao, A novel composite material UiO-66@HNT/Pebax mixed matrix membranes for enhanced CO_2/N_2 separation, Membranes 11 (9) (2021) 693.

[132] J. Yuan, H. Zhu, J. Sun, Y. Mao, G. Liu, W. Jin, Novel ZIF-300 mixed-matrix membranes for efficient CO_2 capture, ACS Appl. Mater. Interfaces 9 (44) (2017) 38575–38583.

[133] Z. Wang, J. Yuan, R. Li, H. Zhu, J. Duan, Y. Guo, G. Liu, W. Jin, ZIF-301 MOF/6FDA-DAM polyimide mixed-matrix membranes for CO_2/CH_4 separation, Sep. Purif. Technol. 264 (2021), 118431.

[134] J. Qian, E. Song, H. Lian, J. Jiang, C. Wang, Y. Pan, High-performance ZIF-302 mixed-matrix membranes for efficient CO_2 capture, Kor. J. Chem. Eng. 39 (4) (2022) 1020–1027.

[135] L. Xiang, L. Sheng, C. Wang, L. Zhang, Y. Pan, Y. Li, Amino-functionalized ZIF-7 nanocrystals: improved intrinsic separation ability and interfacial compatibility in mixed-matrix membranes for CO_2/CH_4 separation, Adv. Mater. 29 (32) (2017), 1606999.

[136] J. Sun, Q. Li, G. Chen, J. Duan, G. Liu, W. Jin, MOF-801 incorporated PEBA mixed-matrix composite membranes for CO_2 capture, Sep. Purif. Technol. 217 (2019) 229–239.

[137] W. Chen, Z. Zhang, L. Hou, C. Yang, H. Shen, K. Yang, Z. Wang, Metal-organic framework MOF-801/PIM-1 mixed-matrix membranes for enhanced CO_2/N_2 separation performance, Sep. Purif. Technol. 250 (2020), 117198.

[138] S. Xu, H. Huang, X. Guo, Z. Qiao, C. Zhong, Highly selective gas transport channels in mixed matrix membranes fabricated by using water-stable Cu-BTC, Sep. Purif. Technol. 257 (2021), 117979.

[139] C. Wu, H. Guo, X. Liu, B. Zhang, Mixed matrix membrane comprising glycine grafted CuBTC for enhanced CO_2 separation performances with excellent stability under humid atmosphere, Sep. Purif. Technol. 295 (2022), 121287.

[140] Q. Qian, A.M. Wright, H. Lee, M. Dincă, Z.P. Smith, Low-temperature $H_2S/CO_2/CH_4$ separation in mixed-matrix membranes containing MFU-4, Chem. Mater. 33 (17) (2021) 6825–6831.

[141] S.J. Datta, A. Mayoral, N.M.S. Bettahalli, P.M. Bhatt, M. Karunakaran, I.D. Carja, D. Fan, P.G.M. Mileo, R. Semino, G. Maurin, O. Terasaki, M. Eddaoudi, Rational design of mixed-matrix metal-organic framework membranes for molecular separations, Science 376 (6597) (2022) 1080–1087.

[142] B. Wang, Z. Qiao, J. Xu, J. Wang, X. Liu, S. Zhao, Z. Wang, M.D. Guiver, Unobstructed ultrathin gas transport channels in composite membranes by interfacial self-assembly, Adv. Mater. 32 (22) (2020), 1907701.

[143] X. Liu, N.K. Demir, Z. Wu, K. Li, Highly water-stable zirconium metal-organic framework UiO-66 membranes supported on alumina hollow fibers for desalination, J. Am. Chem. Soc. 137 (22) (2015) 6999–7002.

[144] X. Liu, H. Jin, Y. Li, H. Bux, Z. Hu, Y. Ban, W. Yang, Metal–organic framework ZIF-8 nanocomposite membrane for efficient recovery of furfural via pervaporation and vapor permeation, J. Membr. Sci. 428 (2013) 498–506.

[145] X. Wang, L. Zhai, Y. Wang, R. Li, X. Gu, Y.D. Yuan, Y. Qian, Z. Hu, D. Zhao, Improving water-treatment performance of zirconium metal-organic framework membranes by postsynthetic defect healing, ACS Appl. Mater. Interfaces 9 (43) (2017) 37848–37855.

[146] Z. Dai, V. Loining, J. Deng, L. Ansaloni, L. Deng, Poly(1-trimethylsilyl-1-propyne)-Based hybrid membranes: effects of various nanofillers and feed gas humidity on CO_2 permeation, Membranes 8 (3) (2018) 76.

[147] H. Jiang, L. Bai, Z. Wang, W. Zheng, B. Yang, S. Zeng, X. Zhang, X. Zhang, Mixed matrix membranes containing Cu-based metal organic framework and functionalized ionic liquid for efficient NH3 separation, J. Membr. Sci. 659 (2022).

[148] C.H. Lau, P.T. Nguyen, M.R. Hill, A.W. Thornton, K. Konstas, C.M. Doherty, R. J. Mulder, L. Bourgeois, A.C.Y. Liu, D.J. Sprouster, J.P. Sullivan, T.J. Bastow, A. J. Hill, D.L. Gin, R.D. Noble, Ending aging in super glassy polymer membranes, Angew. Chem. Int. Ed. 53 (21) (2014) 5322–5326.

[149] A.A. Shamsabadi, R.M. Behbahani, F. Seidi, M. Soroush, Physical aging of polyetherimide membranes, J. Nat. Gas Sci. Eng. 27 (2015) 651–660.

[150] A. Husna, I. Hossain, O. Choi, S.M. Lee, T.H. Kim, Efficient CO_2 separation using a PIM-PI-functionalized UiO-66 MOF incorporated mixed matrix membrane in a PIM-PI-1 polymer, Macromol. Mater. Eng. 306 (10) (2021).

[151] C. Geng, Y. Sun, Z. Zhang, Z. Qiao, C. Zhong, Mitigated aging in a defective metal–organic framework pillared polymer of an intrinsic porosity hybrid membrane for efficient gas separation, ACS Sustain. Chem. Eng. 10 (11) (2022) 3643–3650.

[152] Z. Wang, Y. Tian, W. Fang, B.B. Shrestha, M. Huang, J. Jin, Constructing strong interfacial interactions under mild conditions in mof incorporated mixed matrix Membranes for Gas Separation, ACS Appl. Mater. Interfaces 13 (2021) 3166–3174.

[153] M.Z. Ahmada, T.A. Petersd, N.M. Konnertze, T. Vissere, C. Téllezc, J. Coronasc, V. Filaa, W.M.d. Vosb, N.E. Benes, High-pressure CO_2/CH_4 separation of Zr-MOFs based mixed matrix membranes, Sep. Purif. Technol. 230 (2020), 115858.

[154] M. Rubio-Martinez, C. Avci-Camur, A.W. Thornton, I. Imaz, D. Maspoch, M. R. Hill, New synthetic routes towards MOF production at scale, Chem. Soc. Rev. 46 (11) (2017) 3453–3480.

[155] Q. Min Wang, D. Shen, M. Bülow, M. Ling Lau, S. Deng, F.R. Fitch, N.O. Lemcoff, J. Semanscin, Metallo-organic molecular sieve for gas separation and purification, Microporous Mesoporous Mater. 55 (2) (2002) 217–230.

[156] N. Stock, S. Biswas, Synthesis of metal-organic frameworks (MOFs): routes to various MOF topologies, morphologies, and composites, Chem. Rev. 112 (2) (2012) 933–969.

[157] Y.-K. Seo, J.W. Yoon, J.S. Lee, U.H. Lee, Y.K. Hwang, C.-H. Jun, P. Horcajada, C. Serre, J.-S. Chang, Large scale fluorine-free synthesis of hierarchically porous iron(III) trimesate MIL-100(Fe) with a zeolite MTN topology, Microporous Mesoporous Mater. 157 (2012) 137–145.

[158] A.U. Czaja, N. Trukhan, U. Müller, Industrial applications of metal–organic frameworks, Chem. Soc. Rev. 38 (5) (2009) 1284–1293.

[159] S.H. Jhung, J.-H. Lee, J.-S. Chang, Microwave synthesis of a nanoporous hybrid material, chromium trimesate, Bull. Kor. Chem. Soc. 26 (6) (2005) 880–881.

[160] S.H. Jhung, J.-H. Lee, J.W. Yoon, C. Serre, G. Férey, J.-S. Chang, Microwave synthesis of chromium terephthalate MIL-101 and its benzene sorption, Ability 19 (1) (2007) 121–124.

[161] Z. Ni, R.I. Masel, Rapid production of Metal−Organic frameworks via microwave-assisted solvothermal synthesis, J. Am. Chem. Soc. 128 (38) (2006) 12394–12395.

[162] J.-S. Choi, W.-J. Son, J. Kim, W.-S. Ahn, Metal–organic framework MOF-5 prepared by microwave heating: factors to be considered, Microporous Mesoporous Mater. 116 (1–3) (2008) 727–731.

[163] P.P. Bag, X.-S. Wang, R. Cao, Microwave-assisted large scale synthesis of lanthanide metal–organic frameworks (Ln-MOFs), having a preferred conformation and photoluminescence properties, Dalton Trans. 44 (26) (2015) 11954–11962.

[164] M. Taddei, P.V. Dau, S.M. Cohen, M. Ranocchiari, J.A. van Bokhoven, F. Costantino, S. Sabatini, R. Vivani, Efficient microwave assisted synthesis of metal–organic framework UiO-66: optimization and scale up, Dalton Trans. 44 (31) (2015) 14019–14026.

[165] Y. Xin, S. Peng, J. Chen, Z. Yang, J. Zhang, Continuous flow synthesis of porous materials, Chin. Chem. Lett. 31 (6) (2020) 170–177.

[166] X. Liu, Metal-organic framework UiO-66 membranes, Front. Chem. Sci. Eng. 14 (2) (2019) 216–232.

[167] R. Ameloot, F. Vermoortele, W. Vanhove, M.B. Roeffaers, B.F. Sels, D.E. De Vos, Interfacial synthesis of hollow metal-organic framework capsules demonstrating selective permeability, Nat. Chem. 3 (5) (2011) 382–387.

[168] M. Gimeno-Fabra, A.S. Munn, L.A. Stevens, T.C. Drage, D.M. Grant, R. J. Kashtiban, J. Sloan, E. Lester, R.I. Walton, Instant MOFs: continuous synthesis of metal–organic frameworks by rapid solvent mixing, Chem. Commun. 48 (86) (2012) 10642–10644.

[169] A.S. Munn, P.W. Dunne, S.V.Y. Tang, E.H. Lester, Large-scale continuous hydrothermal production and activation of ZIF-8, Chem. Commun. 51 (64) (2015) 12811–12814.

[170] M. Rubio-Martinez, T.D. Hadley, M.P. Batten, K. Constanti-Carey, T. Barton, D. Marley, A. Monch, K.S. Lim, M.R. Hill, Scalability of continuous flow production of metal-organic frameworks, ChemSusChem 9 (9) (2016) 938–941.

[171] P.M. Schoenecker, G.A. Belancik, B.E. Grabicka, K.S. Walton, Kinetics study and crystallization process design for scale-up of UiO-66-NH_2 synthesis, AIChE J. 59 (4) (2013) 1255–1262.

[172] M. Taddei, D.A. Steitz, J.A. van Bokhoven, M. Ranocchiari, Continuous-flow microwave synthesis of metal–organic frameworks: a highly efficient method for large-scale production, Chem. Eur J. 22 (10) (2016) 3245–3249.

[173] H. Reinsch, S. Waitschat, S.M. Chavan, K.P. Lillerud, N. Stock, A facile "green" route for scalable batch production and continuous synthesis of zirconium MOFs, Eur. J. Inorg. Chem. 27 (2016) 4490–4498, 2016.

[174] A. Laybourn, A.M. López-Fernández, I. Thomas-Hillman, J. Katrib, W. Lewis, C. Dodds, A.P. Harvey, S.W. Kingman, Combining continuous flow oscillatory baffled reactors and microwave heating: process intensification and accelerated synthesis of metal-organic frameworks, Chem. Eng. J. 356 (2019) 170–177.

[175] A. Carne-Sanchez, I. Imaz, M. Cano-Sarabia, D. Maspoch, A spray-drying strategy for synthesis of nanoscale metal-organic frameworks and their assembly into hollow superstructures, Nat. Chem. 5 (3) (2013) 203–211.

[176] C. Avci-Camur, J. Troyano, J. Pérez-Carvajal, A. Legrand, D. Farrusseng, I. Imaz, D. Maspoch, Aqueous production of spherical Zr-MOF beads via continuous-flow spray-drying, Green Chem. 20 (4) (2018) 873–878.

[177] A. Pichon, A. Lazuen-Garay, S.L. James, Solvent-free synthesis of a microporous metal–organic framework, CrystEngComm 8 (3) (2006) 211–214.

[178] D. Crawford, J. Casaban, R. Haydon, N. Giri, T. McNally, S.L. James, Synthesis by extrusion: continuous, large-scale preparation of MOFs using little or no solvent, Chem. Sci. 6 (3) (2015) 1645–1649.

[179] S. Karak, S. Kandambeth, B.P. Biswal, H.S. Sasmal, S. Kumar, P. Pachfule, R. Banerjee, Constructing ultraporous covalent organic frameworks in seconds via an organic terracotta process, J. Am. Chem. Soc. 139 (5) (2017) 1856–1862.

[180] C. Echaide-Górriz, C. Clément, F. Cacho-Bailo, C. Téllez, J. Coronas, New strategies based on microfluidics for the synthesis of metal–organic frameworks and their membranes, J. Mater. Chem. A 6 (14) (2018) 5485–5506.

[181] A. Polyzoidis, T. Altenburg, M. Schwarzer, S. Loebbecke, S. Kaskel, Continuous microreactor synthesis of ZIF-8 with high space–time-yield and tunable particle size, Chem. Eng. J. 283 (2016) 971–977.

[182] C. McKinstry, R.J. Cathcart, E.J. Cussen, A.J. Fletcher, S.V. Patwardhan, J. Sefcik, Scalable continuous solvothermal synthesis of metal organic framework (MOF-5) crystals, Chem. Eng. J. 285 (2016) 718–725.

[183] L. Garzón-Tovar, M. Cano-Sarabia, A. Carné-Sánchez, C. Carbonell, I. Imaz, D. Maspoch, A spray-drying continuous-flow method for simultaneous synthesis and shaping of microspherical high nuclearity MOF beads, React. Chem. Eng. 1 (5) (2016) 533–539.

[184] B. He, M.M. Sadiq, M.P. Batten, K. Suzuki, M. Rubio-Martinez, J. Gardiner, M. R. Hill, Continuous flow synthesis of a Zr magnetic framework composite for post-combustion CO_2 capture, Chem. Eur J. 25 (57) (2019) 13184–13188.

[185] L. Yan, H. Jiang, Y. Wang, L. Li, X. Gu, P. Dai, D. Liu, S.-F. Tang, G. Zhao, X. Zhao, K.M. Thomas, One-step and scalable synthesis of Ni_2P nanocrystals encapsulated in N,P-codoped hierarchically porous carbon matrix using a bipyridine and phosphonate linked nickel metal–organic framework as highly efficient electrocatalysts for overall water splitting, Electrochim. Acta 297 (2019) 755–766.

[186] Y. Wang, L. Li, L. Yan, L. Cao, P. Dai, X. Gu, X. Zhao, Continuous synthesis for zirconium metal-organic frameworks with high quality and productivity via microdroplet flow reaction, Chin. Chem. Lett. 29 (6) (2018) 849–853.

[187] C. McKinstry, E.J. Cussen, A.J. Fletcher, S.V. Patwardhan, J. Sefcik, Scalable continuous production of high quality HKUST-1 via conventional and microwave heating, Chem. Eng. J. 326 (2017) 570–577.

[188] G.H. Albuquerque, R.C. Fitzmorris, M. Ahmadi, N. Wannenmacher, P. K. Thallapally, B.P. McGrail, G.S. Herman, Gas–liquid segmented flow microwave-assisted synthesis of MOF-74(Ni) under moderate pressures, CrystEngComm 17 (29) (2015) 5502–5510.

[189] M. Gaab, N. Trukhan, S. Maurer, R. Gummaraju, U. Müller, The progression of Al-based metal-organic frameworks – from academic research to industrial production and applications, Microporous Mesoporous Mater. 157 (2012) 131–136.

[190] M. Mubashir, Y.Y. Fong, C.T. Leng, L.K. Keong, Issues and current trends of hollow-fiber mixed-matrix membranes for CO_2 separation from N_2 and CH_4, Chem. Eng. Technol. 41 (2) (2018) 235–252.

[191] W. Quan, H.E. Holmes, F. Zhang, B.L. Hamlett, M.G. Finn, C.W. Abney, M. T. Kapelewski, S.C. Weston, R.P. Lively, W.J. Koros, Scalable Formation of diamine-appended metal-organic framework hollow fiber sorbents for postcombustion CO_2 capture, J. Am. Chem. Soc. Au 2 (6) (2022) 1350–1358.

[192] A.K. Zulhairun, Z.G. Fachrurrazi, M. Nur Izwanne, A.F. Ismail, Asymmetric hollow fiber membrane coated with polydimethylsiloxane–metal organic framework hybrid layer for gas separation, Sep. Purif. Technol. 146 (2015) 85–93.

[193] H. Demir, G.O. Aksu, H.C. Gulbalkan, S. Keskin, MOF membranes for CO_2 capture: past, present and future, Carbon Capture Sci. Technol. 2 (2022).

[194] Q. Ma, T. Zhang, B. Wang, Shaping of metal-organic frameworks, a critical step toward industrial applications, Matter 5 (4) (2022) 1070–1091.

[195] N. Sunder, Y.Y. Fong, M.A. Bustam, N.H. Suhaimi, Development of amine-functionalized metal-organic frameworks hollow fiber mixed matrix membranes for CO_2 and CH_4 separation: a review, Polymers (Basel) 14 (7) (2022).

[196] Q.-C. Xia, M.-L. Liu, X.-L. Cao, Y. Wang, W. Xing, S.-P. Sun, Structure design and applications of dual-layer polymeric membranes, J. Membr. Sci. 562 (2018) 85–111.

[197] Y. Tian, Z. Wang, L. Wang, Hollow fibers: from fabrication to applications, Chem. Commun. 57 (73) (2021) 9166–9177.

[198] A.L. Ahmad, T.A. Otitoju, B.S. Ooi, Hollow fiber (HF) membrane fabrication: a review on the effects of solution spinning conditions on morphology and performance, J. Ind. Eng. Chem. 70 (2019) 35–50.

[199] W. Li, P. Su, Z. Li, Z. Xu, F. Wang, H. Ou, J. Zhang, G. Zhang, E. Zeng, Ultrathin metal–organic framework membrane production by gel–vapour deposition, Nat. Commun. 8 (1) (2017).

[200] S. Basu, A. Cano-Odena, I.F.J. Vankelecom, MOF-containing mixed-matrix membranes for CO_2/CH_4 and CO_2/N_2 binary gas mixture separations, Sep. Purif. Technol. 81 (1) (2011) 31–40.

[201] J. Hu, H. Cai, H. Ren, Y. Wei, Z. Xu, H. Liu, Y. Hu, Mixed-Matrix-Membrane-hollow-fibers-of-$Cu_3(btc)_2$-mof-and-polyimide-for-gas-separation-and-adsorption.pdf&gt, Ind. Eng. Chem. Res. 49 (2010) 12605–12612.

[202] P.D. Sutrisna, J. Hou, M.Y. Zulkifli, H. Li, Y. Zhang, W. Liang, M. Deanna, D`Alessandro, V. Chen, Surface functionalized UiO-66/Pebax-based ultrathin composite hollow fiber gas separation membranes, J. Mater. Chem. A 6 (3) (2018) 918–931.

[203] G. Li, W. Kujawski, K. Knozowska, J. Kujawa, Thin film mixed matrix hollow fiber membrane fabricated by incorporation of amine functionalized metal-organic framework for CO_2/N_2 separation, Materials (Basel) 14 (12) (2021).

[204] Y. Dai, J.R. Johnson, O. Karvan, D.S. Sholl, W.J. Koros, Ultem®/ZIF-8 mixed matrix hollow fiber membranes for CO_2/N_2 separations, J. Membr. Sci. 401–402 (2012) 76–82.

[205] B. Sasikumar, S. Bisht, G. Arthanareeswaran, A.F. Ismail, M.H.D. Othman, Performance of polysulfone hollow fiber membranes encompassing ZIF-8, SiO_2/ZIF-8, and amine-modified SiO_2/ZIF-8 nanofillers for CO_2/CH_4 and CO_2/N_2 gas separation, Sep. Purif. Technol. 264 (2021).

[206] N. Widiastuti, T. Gunawan, H. Fansuri, W.N.W. Salleh, A.F. Ismail, N. Sazali, P84/ZCC hollow fiber mixed matrix membrane with PDMS coating to enhance air separation performance, Membranes (Basel) 10 (10) (2020).

[207] O.E.M. Ter Beek, M.K. van Gelder, C. Lokhorst, D.H.M. Hazenbrink, B. H. Lentferink, K.G.F. Gerritsen, D. Stamatialis, In vitro study of dual layer mixed matrix hollow fiber membranes for outside-in filtration of human blood plasma, Acta Biomater. 123 (2021) 244–253.

[208] R. Kamaludin, M. Xuefeng, M.H.D. Othman, A. Imtiaz, M. Hafiz Puteh, S.H.S. A. Kadir, ZIF-8-based dual layer hollow fiber mixed matrix membrane for natural gas purification, Fuel 354 (2023).

[209] M.-L. Liu, Z.-J. Fu, S.-P. Sun, Chapter 12 - hollow fiber spinning of dual-layer membranes, in: T.-S. Chung, Y. Feng (Eds.), Hollow Fiber Membranes, Elsevier, 2021, pp. 253–274.

[210] D. Li, T.-S. Chung, R. Wang, Morphological aspects and structure control of dual-layer asymmetric hollow fiber membranes formed by a simultaneous co-extrusion approach, J. Membr. Sci. 243 (1–2) (2004) 155–175.

[211] L. Jiang, Fabrication of Matrimid/polyethersulfone dual-layer hollow fiber membranes for gas separation, J. Membr. Sci. 240 (1–2) (2004) 91–103.

[212] C. Echaide-Górriz, J.A. Zapata, M. Etxeberría-Benavides, C. Téllez, J. Coronas, Polyamide/MOF bilayered thin film composite hollow fiber membranes with tuned MOF thickness for water nanofiltration, Sep. Purif. Technol. 236 (2020).

[213] G.-K. Gao, Y.-R. Wang, H.-J. Zhu, Y. Chen, R.-X. Yang, C. Jiang, H. Ma, Y.-Q. Lan, Rapid production of metal–organic frameworks based separators in industrial-level efficiency, Adv. Sci. 7 (24) (2020), 2002190.

[214] A. Knebel, A. Bavykina, S.J. Datta, L. Sundermann, L. Garzon-Tovar, Y. Lebedev, S. Durini, R. Ahmad, S.M. Kozlov, G. Shterk, M. Karunakaran, I.D. Carja, D. Simic, I. Weilert, M. Kluppel, U. Giese, L. Cavallo, M. Rueping, M. Eddaoudi, J. Caro, J. Gascon, Solution processable metal-organic frameworks for mixed matrix membranes using porous liquids, Nat. Mater. 19 (12) (2020) 1346–1353.

[215] D. Poloneeva, S.J. Datta, L. Garzon-Tovar, S. Durini, M. Rueping, M. Eddaoudi, A. Bavykina, J. Gascon, Toward liquid phase processable metal organic frameworks: dream or reality? Acc. Chem. Res. 2 (12) (2021) 1133–1140.

[216] C.S. Diercks, O.M. Yaghi, The atom, the molecule, and the covalent organic framework, Science 355 (6328) (2017) 1585.

[217] N. Huang, P. Wang, D. Jiang, Covalent organic frameworks: a materials platform for structural and functional designs, Nat. Rev. Mater. 1 (10) (2016), 16068.

[218] L.M. Lanni, R.W. Tilford, M. Bharathy, J.J. Lavigne, Enhanced hydrolytic stability of self-assembling alkylated two-dimensional covalent organic frameworks, J. Am. Chem. Soc. 133 (35) (2011) 13975–13983.

[219] Y. Du, K. Mao, P. Kamakoti, B. Wooler, S. Cundy, Q. Li, P. Ravikovitch, D. Calabro, The effects of pyridine on the structure of B-COFs and the underlying mechanism, J. Mater. Chem. A 1 (42) (2013) 13171–13178.

[220] Y. Du, K. Mao, P. Kamakoti, P. Ravikovitch, C. Paur, S. Cundy, Q. Li, D. Calabro, Experimental and computational studies of pyridine-assisted post-synthesis modified air stable covalent-organic frameworks, Chem. Commun. 48 (38) (2012) 4606–4608.

[221] B.P. Biswal, S. Chandra, S. Kandambeth, B. Lukose, T. Heine, R. Banerjee, Mechanochemical synthesis of chemically stable isoreticular covalent organic frameworks, J. Am. Chem. Soc. 135 (14) (2013) 5328–5331.

[222] S.Y. Ding, J. Gao, Q. Wang, Y. Zhang, W.G. Song, C.Y. Su, W. Wang, Construction of covalent organic framework for catalysis: Pd/COF-LZU1 in Suzuki-Miyaura coupling reaction, J. Am. Chem. Soc. 133 (49) (2011) 19816–19822.

[223] Z. Li, Y. Zhang, H. Xia, Y. Mu, X. Liu, A robust and luminescent covalent organic framework as a highly sensitive and selective sensor for the detection of Cu^{2+} ions, Chem. Commun. 52 (39) (2016) 6613–6616.

[224] H. Xu, J. Gao, D. Jiang, Stable, crystalline, porous, covalent organic frameworks as a platform for chiral organocatalysts, Nat. Chem. 7 (11) (2015) 905–912.

[225] X. Guan, H. Li, Y. Ma, M. Xue, Q. Fang, Y. Yan, V. Valtchev, S. Qiu, Chemically stable polyarylether-based covalent organic frameworks, Nat. Chem. 11 (2019) 587–594.

[226] Z. Kang, Y. Peng, Y. Qian, D. Yuan, M.A. Addicoat, T. Heine, Z. Hu, L. Tee, Z. Guo, D. Zhao, Mixed matrix membranes (MMMs) comprising exfoliated 2D covalent organic frameworks (COFs) for efficient CO_2 separation, Chem. Mater. 28 (5) (2016) 1277–1285.

[227] Y. Zhang, L. Ma, Y. Lv, T. Tan, Facile manufacture of COF-based mixed matrix membranes for efficient CO_2 separation, Chem. Eng. J. 430 (2022), 133001.

[228] Y. Cheng, L. Zhai, Y. Ying, Y. Wang, G. Liu, J. Dong, D.Z.L. Ng, S.A. Khan, D. Zhao, Highly efficient CO_2 capture by mixed matrix membranes containing three-dimensional covalent organic framework fillers, J. Mater. Chem. A 7 (9) (2019) 4549–4560.

[229] R. Zhao, H. Wu, L. Yang, Y. Ren, Y. Liu, Z. Qu, Y. Wu, L. Cao, Z. Chen, Z. Jiang, Modification of covalent organic frameworks with dual functions ionic liquids for membrane-based biogas upgrading, J. Membr. Sci. 600 (2020), 117841.

[230] C. Zou, Q. Li, Y. Hua, B. Zhou, J. Duan, W. Jin, Mechanical synthesis of COF nanosheet cluster and its mixed matrix membrane for efficient CO_2 removal, ACS Appl. Mater. Interfaces 9 (34) (2017) 29093–29100.

[231] H. Fan, J. Gu, H. Meng, A. Knebel, ü. Caro, High-Flux membranes based on the covalent organic framework COF-LZU1 for selective dye separation by nanofiltration, Angew. Chem. Int. Ed. 57 (15) (2018) 4083–4087.

[232] X. Shi, A. Xiao, C. Zhang, Y. Wang, Growing covalent organic frameworks on porous substrates for molecule-sieving membranes with pores tunable from ultra- to nanofiltration, J. Membr. Sci. 576 (2019) 116–122.

[233] S. Yuan, X. Li, J. Zhu, G. Zhang, P.V. Puyvelde, B.V.d. Bruggen, Covalent organic frameworks for membrane separation, Chem. Soc. Rev. 48 (10) (2019) 2665–2681.

[234] R. Wang, X. Shi, A. Xiao, W. Zhou, Y. Wang, Interfacial polymerization of covalent organic frameworks (COFs) on polymeric substrates for molecular separations, J. Membr. Sci. 566 (2018) 197–204.

[235] C. Fan, H. Wu, J. Guan, X. You, C. Yang, X. Wang, L. Cao, B. Shi, Q. Peng, Y. Kong, Y. Wu, N.A. Khan, Z. Jiang, Scalable fabrication of crystalline COF membranes from amorphous polymeric membranes, Angew. Chem. Int. Ed. 133 (33) (2021) 18199–18206.

[236] J. Fu, S. Das, G. Xing, T. Ben, V. Valtchev, S. Qiu, Fabrication of COF-MOF composite membranes and their highly selective separation of H_2/CO_2, J. Am. Chem. Soc. 138 (24) (2016) 7673–7680.

[237] S. Das, T. Ben, S. Qiu, V. Valtchev, Two-Dimensional COF-Three-Dimensional MOF dual-layer membranes with unprecedentedly high H_2/CO_2 selectivity and ultrahigh gas permeabilities, ACS Appl. Mater. Interfaces 12 (47) (2020) 52899–52907.

[238] H. Fan, A. Mundstock, A. Feldhoff, A. Knebel, J. Gu, H. Meng, J. Caro, Covalent organic framework-covalent organic framework bilayer membranes for highly selective gas separation, J. Am. Chem. Soc. 140 (32) (2018) 10094–10098.

[239] Y. Ying, S.B. Peh, H. Yang, Z. Yang, D. Zhao, Ultrathin covalent organic framework membranes via a multi-interfacial engineering strategy for gas separation, Adv. Mater. 34 (25) (2022), 2104946.

[240] Y. Ying, M. Tong, S. Ning, S.K. Ravi, S.B. Peh, S.C. Tan, S.J. Pennycook, D. Zhao, Ultrathin two-dimensional membranes assembled by ionic covalent organic nanosheets with reduced apertures for gas separation, J. Am. Chem. Soc. 142 (9) (2020) 4472–4480.

[241] H. Fan, M. Peng, I. Strauss, A. Mundstock, H. Meng, J. Caro, High-Flux vertically aligned 2D covalent organic framework membrane with enhanced hydrogen separation, J. Am. Chem. Soc. 142 (2020) 6872–6877.